Variations in esker morphology and internal architecture record time-transgressive deposition during ice margin retreat in Northern Ireland

Ben J. Stoker[1,2,*], Stephen J. Livingstone[1], Iestyn D. Barr[3], Alastair Ruffell[4], Robert D. Storrar[5], Sam Roberson[6]

[*]Corresponding author

[1] Department of Geography, University of Sheffield, UK, South Yorkshire, Sheffield, Winter Street, S10 2TN

[2] Department of Physical Geography and Geoecology, Charles University, Prague, Czechia

[3] School of Science and the Environment, Manchester Metropolitan University, UK, Manchester, Oxford Road, M15 6BH

[4] School of Natural and Built Environment, Queens University Belfast, UK, Belfast, Elmwood Avenue, BT7 1NN

[5] Department of the Natural and Built Environment, Sheffield Hallam University, UK, Sheffield, Howard Street, S1 1WB

[6] Geological Survey of Northern Ireland, Dundonald House, Belfast, BT4 3SB, UK

Keywords: Eskers, Northern Ireland, morphology, sedimentology, deglaciation, meltwater

Abstract

The architecture and evolution of the subglacial hydrological system plays a key role in modulating ice flow. Eskers provide an opportunity to understand subglacial hydrology at a broader temporal and spatial perspective than contemporary studies. Recent research has established a morphogenetic classification for eskers, but these studies have been limited to topographically simple regions of a single ice sheet. We present an updated map of esker distribution in Northern Ireland based on 5 m resolution elevation data, and a high-resolution map (0.4 m resolution) of the glacial geology of SW Northern Ireland. Ground Penetrating Radar data from four sites along the >20 km long Evishanoran esker system in central Northern Ireland are combined with geomorphological observations to provide an insight into depositional processes and controls on esker formation. Esker architecture indicates two main phases of formation, including an initial stage of high energy flow in a subglacial conduit followed by a final stage of waning flow energy closer to the ice sheet margin. These waning flow energy deposits can be used to reconstruct the ice margin retreat rate and pattern. We identify that local topographic complexity and geological conditions (e.g. fault control) are important controls on subglacial hydrological processes. The broad-scale esker architecture remains the same despite variable esker morphology (planform), while there are significant variations in local topography and

geology. We suggest that this represents local factors controlling esker morphology, as hydrological processes alone cannot explain these variations. This study provides further evidence that morphogenetic relationships cannot be based solely on remote sensing data and must be supported by robust field data, especially where post-glacial processes may distort esker morphology (e.g. peat infilling).

1.0 Introduction

The distribution of meltwater at the base of ice sheets influences ice motion by modulating basal sliding and deformation of sediments. The influence of water on ice flow depends on the architecture of the subglacial drainage network and how it evolves to accommodate water inputs (e.g. Budd et al., 1979; Alley et al., 1986; Iken and Bindshadler, 1986). Efficient low-pressure networks of discrete channels rapidly drain water to the margin and tend to reduce ice velocity (Hubbard and Nienow, 1997). Inefficient distributed networks (e.g. linked cavities, canals and a porous till layer) result in increased effective pressure, in turn leading to higher ice velocities (Röthlisberger, 1972; Schoof, 2010). Recent observations from beneath the Antarctic and Greenland ice sheets have implicated dynamic subglacial water systems in driving rapid ice-flow variations (Zwally et al., 2002; Bell et al., 2007; Stearns et al., 2008; Bartholomew et al., 2010; Davison et al., 2019).

For investigations of subglacial hydrological processes, the imprint of meltwater drainage, recorded on the beds of former ice sheets, has a clear advantage over data from contemporary ice sheets (e.g. borehole surveys) because it is possible to reconstruct the history of meltwater drainage over centennial to millennial time-scales and spatially over metres to hundreds of kilometres. These temporal and spatial scales not only allow a more complete understanding of the architecture and evolution of the subglacial drainage network but are relevant for informing numerical modelling experiments (cf. Greenwood et al., 2016; Hewitt & Creyts, 2019). Eskers are the depositional imprint of drainage through subglacial (R-channels), englacial or supraglacial channels (Price, 1969; Banerjee and McDonald, 1975; Gustavson and Boothroyd, 1987; Brennand, 2000) and are commonly found across the beds of former ice sheets (e.g. Storrar et al., 2014a; Stroeven et al., 2016; Clark et al., 2018). They typically comprise elongate ridges of fluvioglacially deposited sand and gravel that can extend tens to hundreds of kilometres, are arranged roughly parallel to former ice flow direction, and range from single ridges to more complex anabranching forms (e.g. Flint, 1930; Brennand, 1994; Burke et al., 2012; Storrar et al., 2015; Perkins et al., 2016). Esker geometry, distribution and sedimentary architecture have been widely used to reconstruct drainage pathways and infer past ice sheet dimensions and dynamics (e.g. Shreve, 1985; Dyke and Prest, 1987; Aylsworth and Shilts, 1989; Hebrand and Åmark, 1989; Clark and Walder, 1994; Brennand, 1994, 2000; Warren and Ashley, 1994; Margold et al., 2013; Storrar et al., 2013, 2014a; Livingstone et al., 2015). However, there is still considerable uncertainty over the genesis of eskers, including the extent to which they form time-transgressively or synchronously (e.g. Brennand,

2000; Makinen, 2003; Cummings et al., 2011); the magnitude and frequency of drainage (Burke et al., 2008, 2010, 2012; Livingstone et al., 2016; Drews et al., 2017); and the vertical position in the ice mass (i.e. supraglacial, englacial or subglacial) in which they are deposited (Price, 1969; Fitzsimmons, 1991; Perkins et al., 2016).

Understanding how eskers form is important for reconstructing palaeo-ice sheets and providing information on subglacial hydrological processes. In particular, the varied form and architecture of eskers is thought to be controlled by the hydrological properties of the channelised drainage system (Burke et al., 2015; Storrar et al., 2015). For example, recent morpho-sedimentary studies of eskers in southern Alberta, Canada, and mapping of eskers emerging from the front of Breiðamerkurjökull, southeast Iceland, have related abundant meltwater and sediment supply to complex esker systems, and low sediment supply and either high or low meltwater abundance to single ridges of uniform geometry (Burke et al., 2015; Storrar et al., 2015, 2020). A barrier to understanding the formation of eskers at the ice sheet-scale is the relative dearth of sedimentological investigations of these long esker systems. Recent work (e.g. Burke et al., 2012; Perkins et al., 2013) has begun to address this using geophysical investigations of the sedimentary architecture of eskers formed beneath the Cordilleran Ice Sheet. To further investigate the relationship between ice sheet hydrology and esker properties, this paper combines detailed geomorphological, geophysical and sedimentological data to assess controls on the formation of a ~20 km long esker network in Northern Ireland (UK) whose morphology changes down-flow from a complex multi-ridge system to a large single ridge.

2.0 Background

2.1 Glacial history of Ireland

The early stages of the onset of the Irish Ice Sheet (~ 35 ka) were characterised by incursion of Scottish ice flowing in from the NE, which subsumed localised ice caps over Irish upland massifs (Colhoun, 1971; Clark and Meehan, 2001; Greenwood and Clark, 2009b). As Irish ice coalesced with western Scottish ice, the location of the dominant ice dispersal centres migrated to upland areas in the west of Ireland, exerting a strong control on ice flows patterns (Greenwood and Clark, 2009b). Heterogenous growth patterns led to ice sheet sectors reaching their maxima at different times. For example, the western margin reached its maximum position relatively early compared to the southern portion of the ice sheet (Ó Cofaigh and Evans, 2007; Greenwood and Clark, 2009b; Ó Cofaigh et al., 2019). The configuration of ice domes and the geomorphology of the Irish Ice Sheet required ice expansion onto the continental shelf, with the Last Glacial Maximum (LGM; 23 ka – 18 ka) resulting in almost complete terrestrial ice coverage across Ireland (Knight et al., 2004; Ó Cofaigh and Evans, 2007; Bradwell et al., 2008; Greenwood and Clark, 2009a,b; Clark et al. 2018).

Deglaciation in Ireland was characterised by the migration of competing ice divides, which resulted in a complex deglacial history (Knight, 2003, 2019; Greenwood, 2009b). The ice sheet fragmented as it retreated into upland dispersal centres such as the Connemara Mountains in Western Ireland and County Donegal to the north (Wilson *et al.*, 2019), or lowland ice domes situated in the Lough Neagh Basin and Omagh Basin (Fig. 1). Ice sheet retreat is thought to have been interspersed with asynchronous phases of localised ice advance or stagnation, likely related to the migration of ice divides (Knight, 1999; Knight, 2006; Clark *et al.*, 2012; Chiverrell *et al.*, 2020). Within central Northern Ireland, the two dominant LGM ice dispersal centres were situated in the Lough Neagh basin, and in the Sperrin Mountain range to the north (Fig. 1) (Knight, 1999). During this period, SW ice flow dominated from an ice dome in the NE Omagh Basin offshore towards the Donegal Bay (Fig. 1), indicated by an area of subglacial ribs across the Omagh Basin (Knight and McCabe, 1997). Subglacial ribs across central Northern Ireland often display modification or drumlinisation likely associated with changes in ice flow patterns and subglacial thermal regime (Knight, 1997; Knight and McCabe, 1997). An ice flow reversal occurred during deglaciation when the dominant ice dome over the Omagh Basin migrated SW to the Lower Lough Erne basin, leading to NE ice flow forming a prominent esker system overlying the subglacial ribs (Knight, 2004). The regional retreat pattern to the SW is documented by a series of meltwater landforms, including eskers. The final stages of deglaciation were characterised by localised mountain ice caps, with the last remnants of the Irish Ice Sheet likely located in the mountains of Donegal in the northwest (Greenwood and Clark, 2009b; Smith and Knight, 2011).

Research into the meltwater systems of Ireland has a long history stretching back to the late 19th century, and has concentrated on the origin of the large (up to 50 m high) ridges of the Esker Riada system in the Irish Midlands (Sollas, 1896; Gregory, 1912, 1921; Hinch, 1921; Flint, 1930). Theories on the origin of these eskers revolved around whether they were deposited by a sub- or supraglacial river system, or whether they represented deltaic fluvioglacial deposits (Gregory, 1921). More recently, studies have debated whether the Esker Riada system and associated fluvioglacial sediments were deposited by meltwater in an interlobate position, between two retreating ice masses (Warren and Ashley, 1994; Pellicer et al., 2012), or as part of a multi-phase model involving westerly ice sheet retreat, followed by a period of ice sheet readvance from the north (Delaney, 2001a, b, 2002; Delaney et al., 2018). The eskers of central Northern Ireland have been used to reconstruct the migration of ice domes and time-transgressive variations in the subglacial drainage system (Knight, 1997; 2019), but historically, there has been less research focused on them.

2.2 Regional Context and Landform Distribution

Central Northern Ireland incorporates the Sperrin Mountains to the north and the Omagh Basin; a low elevation region of undulating topography, to the south (Fig. 1). The regional geology is varied, with a series of folded and faulted Palaeozoic sandstones and limestones to the south, and crystalline granites

and gabbros to the north (Knight, 1997; Geological Survey Northern Ireland, 2016). A series of three large, subparallel fault lines trend NE-SW and define geological boundaries, while smaller faults with a variety of orientations are also prevalent (Geological Survey Northern Ireland, 2016).

A range of glacial landforms have been documented across the region, including meltwater channels, eskers, drumlins and subglacial ribs (Colhoun, 1970; Knight, 2003; Clark et al., 2018). Major moraines are largely absent across central Northern Ireland, being restricted to the present coastline and the continental shelf onto which the Irish Ice Sheet extended (Clark et al., 2018). An area of subglacial ribs dominates the lowland areas across Central Northern Ireland, with ridge crestlines oriented perpendicular to SW ice flow during the LGM (Knight and McCabe, 1997; Knight, 2003). These subglacial ribs are commonly drumlinised or exhibit modification by meltwater, which may have been stored in the lowland area between ridge crestlines (Knight and McCabe, 1997; Knight, 2003, 2006). Alongside subglacial ribs, E-W orientated drumlins dominate the lowlands of the Omagh and Lough Erne Basins (Knight, 1997, 2003). A prominent esker system located in the NE of the Lower Lough Erne Basin forms a series of bifurcating ridges in a meltwater valley dissecting the zone of subglacial ribs (Fig. 2a). This system was deposited under NE ice flow during deglaciation to the SW, contrasting with the SW ice flow responsible for the formation of the subglacial ribs. Therefore, these eskers represent a reversal of the hydraulic gradient as the ice dome situated over the Omagh Basin migrated towards the Lower Lough Erne Basin (Knight and McCabe, 1997).

The present study focuses on a >20 km long complex esker system in County Tyrone, Central Northern Ireland. The esker complex trends out of three meltwater channels cutting through the hills to the south, and terminates near the Davagh Forest in the north (Figs. 2 and 3). The NE sector was mapped in part by Gregory (1925) and termed the Evishanoran Esker. Early debate sought to identify whether deposition was associated with local ice masses from the east, or related to a larger ice mass from the southwest (Charlesworth, 1926; Gregory, 1926). Here we refer to the entire esker complex as the Evishanoran Esker, including newly mapped segments that were not documented in Gregory (1925).

3.0 Methods

3.1 Geomorphological mapping

Comprehensive mapping of esker ridges was undertaken for the whole of Northern Ireland. Landform mapping was performed within ArcGIS 10.4.1, using a 5 m resolution digital elevation model (DEM) produced by the Land and Property Services Northern Ireland under MOU205, provided to Queens University Belfast. We also mapped all glacial landforms across the study area of SW Northern Ireland using a ~0.4 m resolution digital surface model (DSM) to provide geomorphological context of the area surrounding the Evishanoran Esker (Fig. 2).

Landform identification was based on morphology, association with other features and local topography. Landforms were digitized as either polylines or polygons. Esker crestlines were digitized as polylines to investigate broad-scale distribution and morphological characteristics. Fan-shaped enlargements located at esker termini were classified as esker fans and digitized as polygons at the break of slope. The thalwegs of meltwater channels were digitized as polylines and classified as either subglacial or lateral according to the criteria set out by Greenwood *et al* (2007). All subglacial bedforms were mapped as polygons, including: subglacial ribs (ribbed moraine), drumlins, mega-scale glacial lineations, and streamlined bedrock features. Our mapping builds on earlier low-resolution mapping from Landsat and SPOT satellite imagery and field surveys (Knight, 2003; Greenwood and Clark, 2009a), and has resulted in the creation of a comprehensive database of Northern Irish eskers, consistent with the NextMap 5 m resolution data used for the rest of the UK (Clark et al., 2018), and detailed mapping of glacial landforms in SW Northern Ireland at 0.4 m resolution.

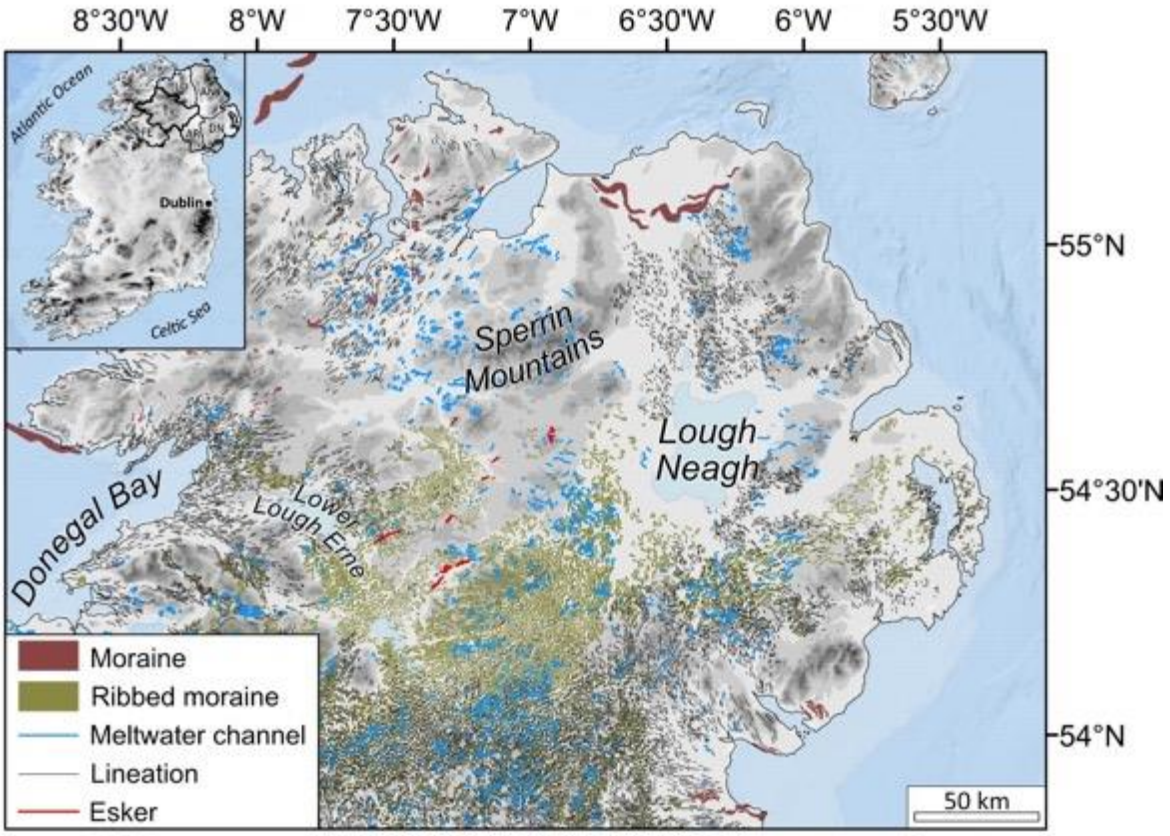

Figure 1. The distribution of mapped glacial landforms within the BRITICE v2 database across Northern Ireland (Clark *et al.*, 2018). Subglacial lineations include Mega-Scale Glacial Lineations and drumlins.

3.2 Ground Penetrating Radar

Ground Penetrating Radar (GPR) data were acquired in August and November 2016. A total of ~1.8 km are presented here, including profiles along the crestlines of the eskers and cross profiles in a range

of topographic contexts and for different esker forms. A 32-bit Mala Ground Explorer (GX) controller unit connected directly to a 160MHz GX shielded antenna on a rough terrain skid plate was used in August 2016. Radar profiles were acquired at a constant walking pace in a continuous, time-triggered shot mode using hyperstacking to reduce random noise. A Mala Ramac system consisting of a 4 m-long Rough Terrain Antenna, comprising in-line, unshielded transmitting and receiving antennas with a 1.5 m spacing and 100MHz centre frequency was used in November 2016. Collection of radar data was performed at a constant walking pace, in a time-triggered mode, with 16 stacks at a delay of 0.5-seconds. All radar survey lines were simultaneously mapped using a Leica CS15 differential Global Positioning System (dGPS) unit to topographically correct the profiles.

Processing of radar data was performed within REFLEXW v7.5.9, the proprietary software of Karl Sandmeier under licence number 401 provided to Queen's University, Belfast. A standard processing sequence was developed, using the following steps: static correction of time-zero drift, removal of low frequency signal saturation (dewow), application of gain to increase the visibility of reflections at depth, diffraction stack migration, background removal to reduce antenna ringing, bandpass filtering and topographic correction with the associated dGPS trace, finally radargrams were plotted in MatLab v9.1.0.441655 (Neal, 2004; Cassidy and Jol, 2009). A velocity of 0.1 m/ns for migration was used, consistent with exposures of eskers in sand extraction pits, hillside scars and road-cuts (see section 3.3) (Russell et al., 2001; Pellicer et al., 2012; Livingstone et al., 2016). GPR profiles were interpreted by identifying high-amplitude reflectors indicative of bounding surfaces between radar facies. Six radar facies (*sensu* Gawthorpe *et al.*, 1993) were differentiated based upon depositional characteristics, including associations with sediment facies identified from exposures in the field and the broad characteristics of reflectors within a unit (Table 1). Lateral discontinuities and offset reflectors were interpreted as geological faults (e.g. Fiore et al., 2002).

3.3 Sedimentology

Gravel pit exposures adjacent to, and below, the GPR profiles were investigated to provide an insight into the flow conditions responsible for ridge formation in the Evishanoran Esker, and to provide ground-truthing for the interpretation of radargrams. Four sediment exposures were logged within the complex, multi-ridge system and the simple, single-ridge system (Fig. 2). Scaled sediment logs were drawn to record stratigraphic data, including details on the sedimentary structures, texture, and the unit characteristics, such as bed geometry and contacts. Lithofacies were based on Evans and Benn (2004). Clast macrofabric and palaeoflow indicators (e.g. ripples) supplemented stratigraphic logs (Miall, 1985).

222 Table 1. Summary of key radar facies observed along the Evishanoran Esker, including both
223 fluvioglacial and post-glacial features. Further description and interpretation of radar facies is presented
224 in section 4.2.1.

Facies type	Radar facies example	Facies characteristics	Facies Interpretation
Esker ridge facies		Radar Facies 1: Chaotic, discontinuous reflectors.	Coarse gravel formed subglacially under high flow velocities (Burke *et al.*, 2015)
		Radar Facies 2: Sub-horizontal, moderately continuous reflectors.	Vertical accretion of fine-grained material (Burke *et al.*, 2012)
		Radar Facies 3: High-angle, downflow dipping reflections.	Fine-grained, foreset deposits (Burke *et al.*, 2010)
		Radar Facies 4: Concave, basin-like reflectors.	Scour-and-fill basins (Perkins *et al.*, 2016)
Post-glacial facies	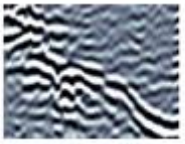	Radar Facies 5: Attenuated, horizontal reflections.	Post-glacial peat infill (Jol and Smith, 1991)

225

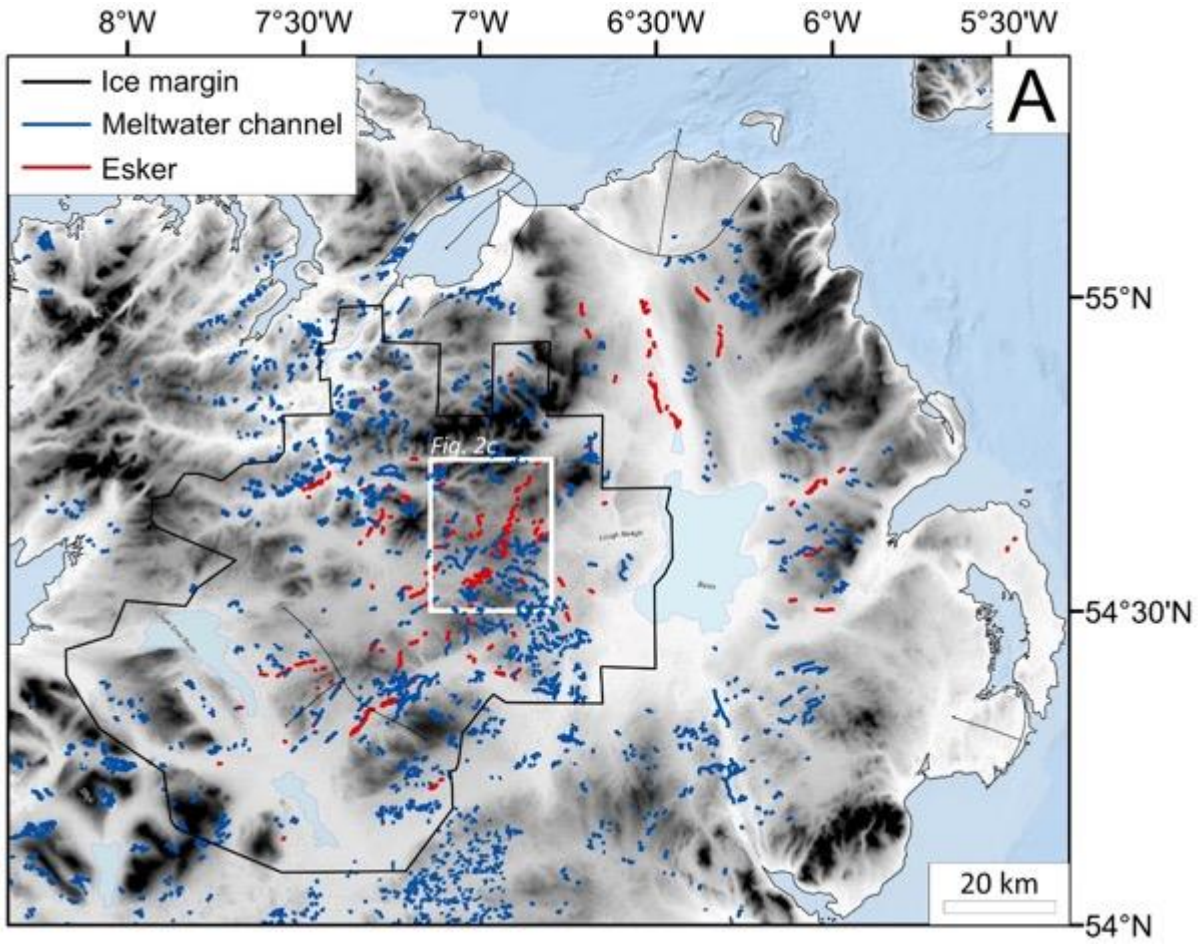

226

227 Figure 2. (a) An updated map of meltwater landforms of Northern Ireland, including features mapped
228 in this study. Meltwater channels from the BRITICE v2 compilation are also included (Clark *et al.*,
229 2018). Note the occurrence of a large esker system to the west of Lough Neagh, unreported in the
230 BRITICE database. Ice margin positions are adapted from Greenwood and Clark (2009b), with arrows
231 showing ice margin retreat direction. The black box indicates the extent of high-resolution (~0.4 m)
232 DSM coverage used within this study and shown in Figure 2b.

233

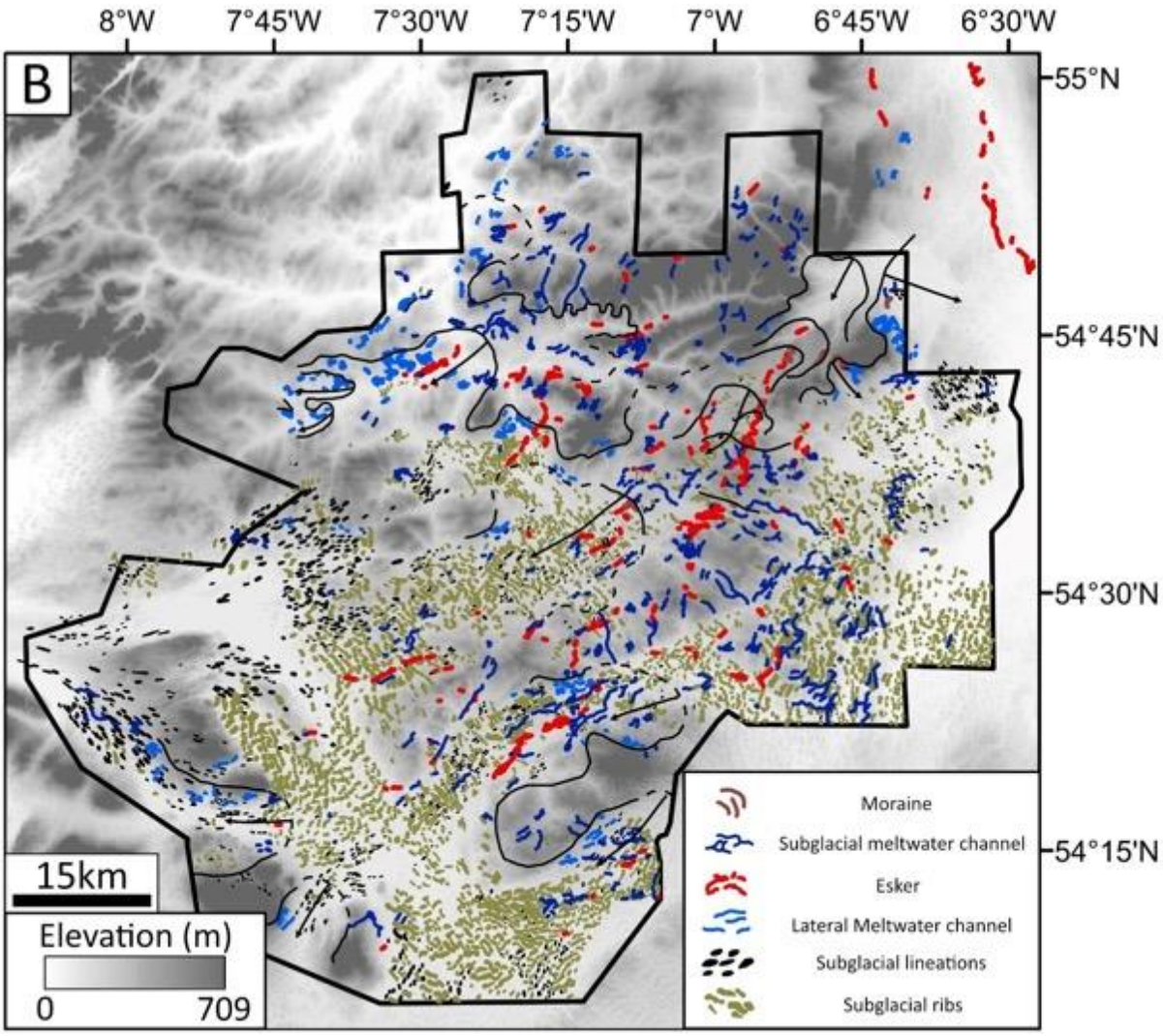

234

235 Figure 2. (b) Glacial geomorphology of SW Northern Ireland based on a 0.4m DSM. Schematic ice
236 margin positions (black lines) have been drawn based on esker morphology, fan deposits, lateral
237 meltwater channels and moraines. Dotted black lines indicate areas of lower certainty in ice margin
238 position. Black arrows indicate ice margin retreat directions. The white outline indicates the extent of
239 DSM coverage.

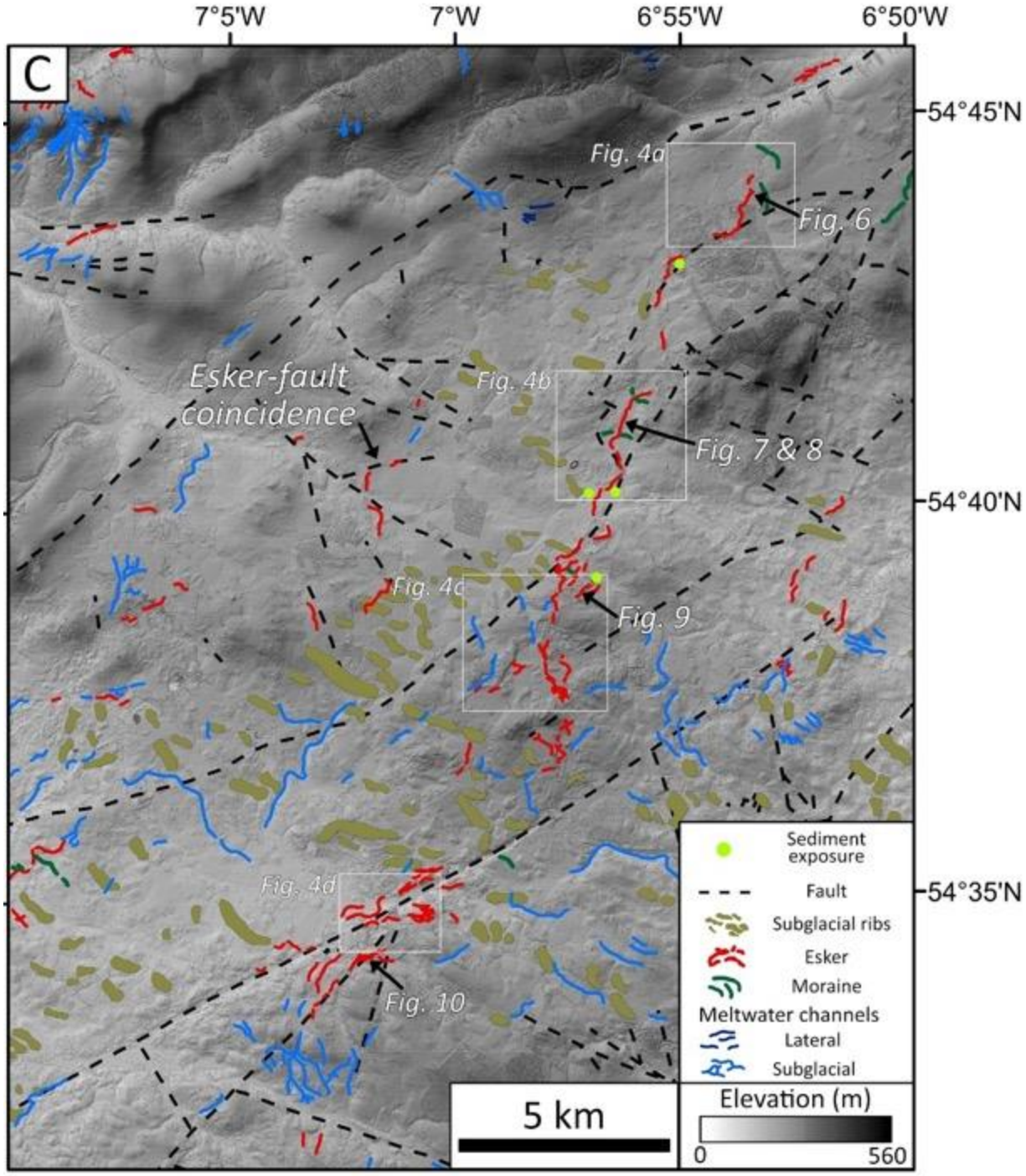

240

241 Fig. 2c. The esker system in County Tyrone, annotated with the location of investigated sediment
242 exposures. Note the coincidence of the southern esker system with a large SW-NE trending fault, while
243 some eskers in the northwest demonstrate dramatic changes in orientation to follow fault lines. White
244 boxes highlight features detailed within Fig. 4. Geological faulting data is based on the 10K geology
245 dataset, reproduced with the permission of the Geological Survey of Northern Ireland. Crown Copyright
246 2018.

4.0 Results and interpretations

4.1 Glacial Geomorphology

A complete map of the glacial meltwater landforms of Northern Ireland is presented in Fig. 2a. The map contains 457 esker ridges, totalling 219.6 km in length, compared to 63 esker ridges (39.4 km) detailed for this region in the BRITICE v2 database (Clark *et al.*, 2018). Esker distribution is heterogenous, with the majority concentrated in a NE-SW axis to the south of the Sperrin Mountains. A > 20 km long N-S trending esker system is present to the north of the Lough Neagh Basin. Meltwater channels most commonly occur near upland regions (Fig. 2a). Meltwater channels have been documented by previous mapping efforts and are ubiquitous across Northern Ireland (Charlesworth, 1924; Colhoun, 1970; Knight, 2006; Greenwood and Clark, 2009a).

We present a detailed map of the glacial geomorphology of SW Northern Ireland in Fig. 2b, including moraines, meltwater channels (lateral and subglacial), eskers and subglacial bedforms (lineations and ribs). To the south of the Sperrin Mountains, a complex system of over 80 ridges form the Evishanoran esker system, spanning > 20 km and demonstrating considerable variation in morphology over its length (Fig. 2 and 3). The esker system is oriented SW-NE, broadly aligned with an area of subglacial ribs. Across this region, further fluvioglacial landforms associated with the esker system are observed. Most notably, the SW sector is associated with a series of subglacial meltwater channels cut into a slope that trends against the regional northwards ice flow, outwash fans are located at the northern terminus of some eskers, and a kame terrace is observed on the southern slopes of the Sperrin Mountains. We define three distinct esker sections based on variations in esker planform; the northern sector of the esker is composed of a predominantly simple system of single ridges, the central sector is dominated by a complex, arborescent ridge network distributed around a hill (~100m relief), and the southern sector comprises a complex, anabranching system of multiple subparallel ridges (Figs. 3, 4).

In the northern sector of the esker system (Fig. 4a,b), a simple planform dominates, consisting of nine consecutive ridges, with a total length of ~9 km (Table 2). The esker system trends uphill towards the NE, with ridges orientated along a uniform, broad valley bottom. However, the eskers in this sector are morphologically complex. Some adjacent ridge segments display an offset relationship, while others terminate in fans at their northern end, or may exhibit enlargements in the esker profile (Fig. 4b; Table 2). These ridges display considerable variability in size; varying from 25 – 80 m in width and from 5 – 15 m in relief. We identify a series of six small moraine ridges across this sector, which record former ice margin standstills. Three of the four esker enlargements and outwash fans are observed in adjacent to a moraine.

Figure 3. Photographs detailing the morphology of the Evishanoran Esker. (A) A photograph looking east along a round-crested ridge within the complex, multi-ridge esker in the southern sector (54.571°N, -7.041°E). (B) An esker ridge within the central sector of the esker complex, formed by water flow down the hill from the right of the image (54.650°N, -6.953°E). (C) A ridge along the Esker Road within the northern sector (54.683°N, -6.942°E). Radar surveys revealed peat infilling around the ridge, masking the true esker size. (D) Large variations in ridge morphology towards the termination of the northern sector (54.734°N, -6.893°E).

Further SW (central sector), the esker transitions into a complex, arborescent system of short ridges (~0.3 km long) with more subdued relief (~6 m). This coincides with a change in the surrounding topography to greater relief variation (183 – 296 m a.s.l.) and a broadly downhill trend towards the NE. The southern end of the esker is split around a hill, with the western limb trending S-N before turning W-E, where it is cross-cut by the eastern limb, which trends N-S (Figs. 2a, 4c). The esker ridges within this sector display a dominantly simple morphology, with an enlargement only observed on a single ridge. We mapped a single moraine within this esker sector.

The southern sector consists of multiple, subparallel ridges along a slope which broadly trends downhill to the NE. While considerable variation in relief is observed due to the undulating terrain, cross-cutting relationships are absent within this sector, although ridges are observed to bifurcate (Fig. 4d). A single small esker enlargement is observed within this sector. A single, small moraine is present at the eastern end of this system.

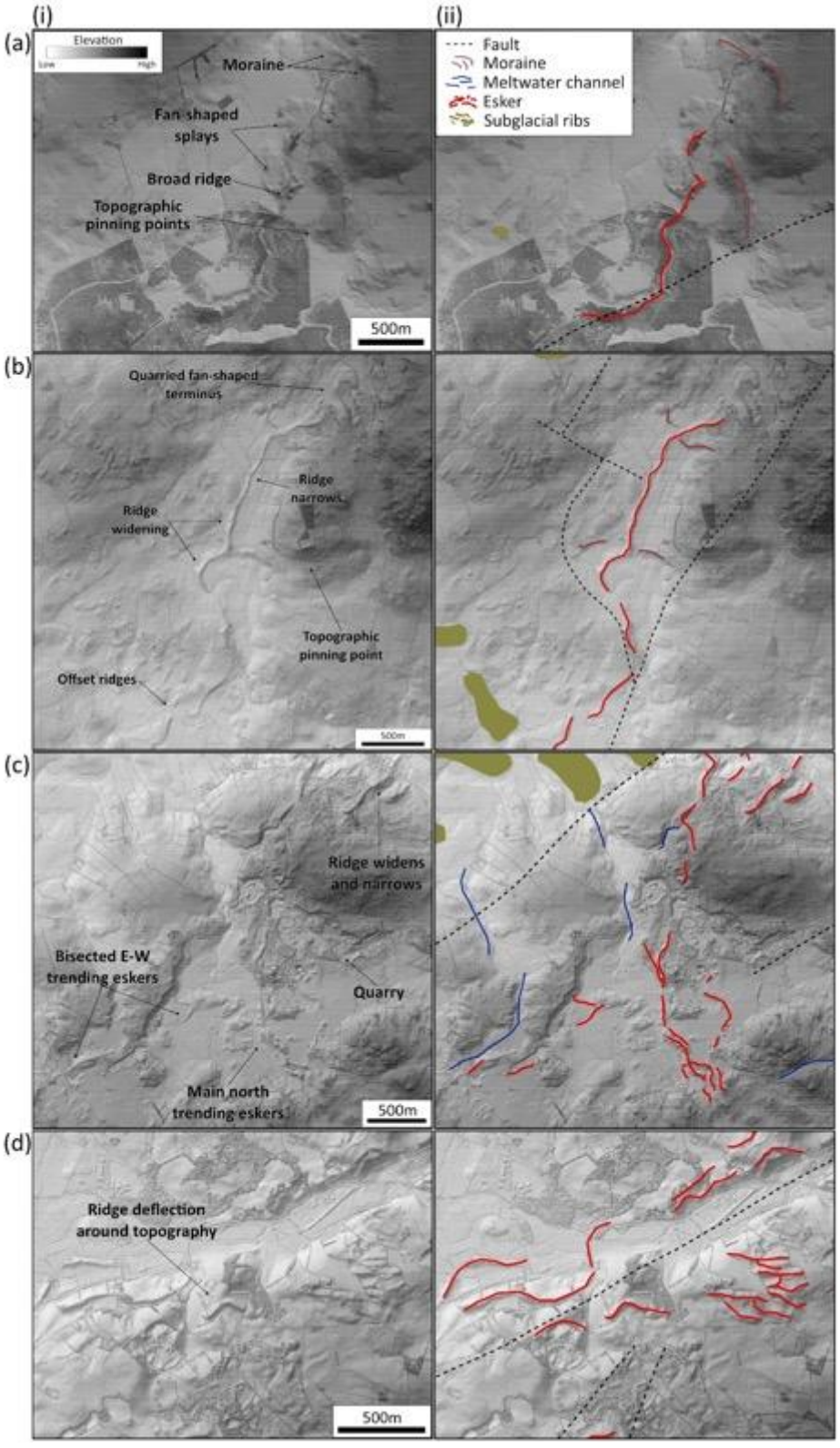

Figure 4. Hillshaded DEM detailing key morphological characteristics of the Evishanoran Esker. (a) Widening of the esker ridge towards the terminus of the simple system in the northern sector, (b) Offset ridges at the initiation of the simple system in the northern sector, (c) Cross-cutting of east trending ridges by the main north trending ridge within the complex esker system in the central sector of the esker complex, (d) Deflection of ridges around a topographic obstacle (possible bedrock or earlier drumlin) within the southern sector.

Complex geological faulting is observed across the study region (Fig. 2). Esker ridges commonly occur near faults, while some also change orientation to follow faultlines (GSNI, 2016) (Fig. 2). This is illustrated by the large fault system towards the S of the region, which trends ENE-WSW; a high concentration of esker ridges within the southern sector of the esker display a spatial correspondence to the fault and run subparallel to it (Fig. 4d). Individual ridges in the central sector of the Evishanoran Esker are coincident with faults, where the main esker trends NE-SW towards the N of the sector. Examples of correspondence between geological faults and eskers are not limited to the Evishanoran Esker: to the west a small series of eskers change orientation to follow a fault which trends NW-SE, highlighted in Figure 2. These changes occur three times over the ~ 5 km length of this esker.

4.2 Esker Internal Architecture

4.2.1 Radar facies (RF) description and interpretation

The GPR radar facies from both shielded 160MHz and unshielded 100MHz Rough Terrain antennas were found to be broadly comparable (see below) and are outlined in Table 1. In this section we describe facies characteristics in detail and interpret the depositional environments.

4.2.1 RF1 – Coarse, poorly-bedded deposits

RF1 often constitutes the core of the esker ridge, forming a tabular unit (up to 10 m thick) of discontinuous, chaotic reflectors subparallel to the bed slope. The lower portion of RF1 often contains hyperbola-generating point reflections. This unit is conformably overlain by RF2 or RF3, or truncated by RF4 (Table 1).

Chaotic facies have been widely attributed to coarse, poorly-sorted deposits (Burke et al., 2008; Pellicer and Gibson, 2011; Franke *et al.*, 2015; Livingstone et al., 2016; Perkins et al., 2016). This is supported by sediment exposures through RF1, which comprise a variety of massive, coarse, gravelly or diamictic deposits interpreted to have formed by the rapid deposition of hyperconcentrated water flows (Fig. 5c; 5d) (Saunderson, 1977; Gorrell and Shaw, 1991; Pellicer and Gibson, 2011; Pellicer et al., 2012; Livingstone et al., 2016). Previous studies consider point reflections to represent out-of-plane boulder clusters and a coarsening of material within the ridge (Burke, 2010; Burke et al., 2012). Out of plane reflections (sideswipes and hyperbola) are observed to be artefacts of upstanding surface objects such as trees, poles and metal farm gates (Neal, 2004). These are most notable on data from the 100MHz unshielded antenna, and thus are disregarded in our interpretations.

4.2.2 RF2 – Horizontally-bedded sands

RF2 generally forms tabular units (~5 m thick) of continuous, subhorizontal reflectors (up to 30 m long) that form parallel to the bed slope (<5° dip from horizontal). It typically forms a central unit in the esker profile, regularly underlain by RF1 and draped by RF3.

Previous studies have attributed similar patterns of subhorizontal reflectors to a flow regime characterised by vertical sediment accretion (Perkins et al., 2016). This interpretation is consistent with sediment exposures through RF2 (Fig. 5a), which suggest horizontally-bedded sands deposited in a low-energy glaciofluvial environment (Banerjee and McDonald, 1975; Burke et al., 2012).

4.2.3 RF3 – Fine-grained, foreset deposits

RF3 forms laterally constrained, wedge-shaped units (2 – 5 m thick) draped over underlying radar facies (Table 1). They comprise a series of onlapping, high-angle (4° - 15° from horizontal), N to NE dipping reflections. RF3 is always the topmost unit where identified and therefore represents the final stage of esker building.

We interpret the steeply dipping reflectors as foreset beds deposited during waning flow conditions (Fiore et al., 2002; Burke et al., 2008, 2010). The absence of associated backset beds suggest that deposition was in a low energy environment (Burke et al., 2010). This is supported by a sediment exposure located NE of a radar survey within a ridge dominated by RF3, documenting a series of fine-grained, cross-stratified and downflow-dipping deposits. The lack of topset structures is indicative of outwash fan-style deposits rather than a deltaic environment (Fig. 5b) (Fiore *et al.*, 2002; Winsemann *et al.*, 2007).

4.2.4 RF4 – Cut-and-fill basins

RF4 is defined by strong, concave-upwards bounding reflectors and subhorizontal to concave internal reflectors (Table 1). The bounding reflectors vary in angle, with the units ranging from narrow, steep-sided basins to broader basin infills, which may extend for up to 60 m along the esker surface and reach thicknesses of up to 10 m. RF4 truncates underlying facies, displaying an erosional, lower bounding surface. Most frequently, RF4 is located near the surface of the esker, but in places is conformably overlain by RF3. RF4 is interpreted as cut-and-fill troughs, formed during the late-stages of esker genesis as water incised into the underlying sediments, and subsequently filled as flow conditions waned (Gorrell and Shaw, 1991; Sambrook-Smith et al., 2006; Perkins et al., 2016).

366 Table 2. The key morphological characteristics of the complex esker system in County Tyrone. The
367 distance along the crestline of each ridge was measured to define the average ridge length. Esker
368 sinuosity was calculated for each individual ridge by dividing the esker ridge length by the straight line
369 distance from esker initiation to terminus, and is presented as a mean for each sector.

	Southern sector	**Central sector**	**Northern sector**
Planform	Complex, multi-ridge	Complex, tributary system	Simple
Average ridge length (m)	357	334	678
Sinuosity	1.17	1.21	1.2
Topographic context	Normal slope through undulating topography	Normal slope through hilly topography	Reverse slope through a uniform valley bottom
Relative relief (m)	~7	~6	~10-15
Total esker length (km)	~6.5 (36 ridges)	~7.4 (39 ridges)	~9.3 (10 ridges)

370

371 *4.2.5 RF5 – Post-glacial infill*

372 Present along the flanks in cross-profile surveys of esker ridges, RF5 is separated from the main esker
373 ridge elements by a strong bounding surface, which dips steeply away from the esker (Table 1). The
374 interior of these units is strongly attenuated and characterised by homogenous reflections which are
375 broadly horizontal. RF5 is interpreted as postglacial infill of the area surrounding the esker ridge. The
376 reflection patterns are consistent with that of peat, which is prevalent across Ireland and confirmed by
377 observations in the field (Jol and Smith, 1991; Pellicer *et al.*, 2012).

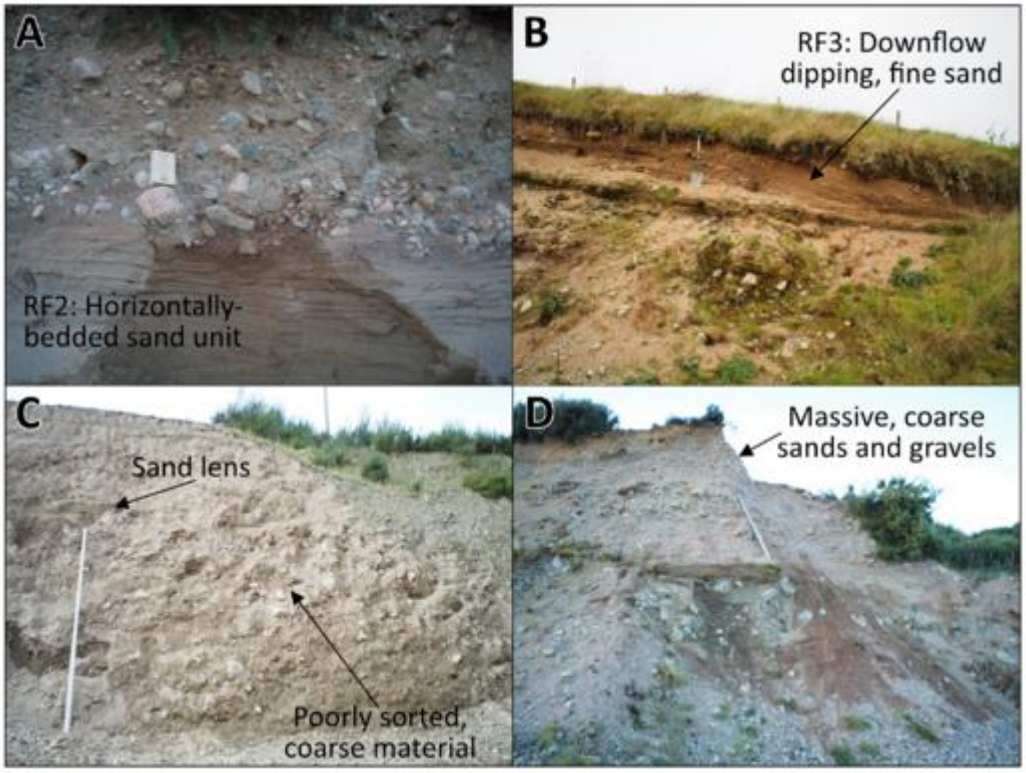

Figure 5. (a) Sediment exposure from the southern-end of the northern sector, consisting of a series of horizontally stratified sands, overlain by a massive gravel unit (54.668°N, -6.950°E). (b) Sediment exposure within the central, complex esker system, dominated by a series of fine-grained, downflow-dipping fan deposits associated with RF3 (54.650°N, -6.953°E). (c) Quarried section of the single esker ridge system to the north of (a). Facies consist of coarse, diamictic material with boulders up to 50 cm (54.672°N, -6.941°E). (d) Massive sand and gravel units observed within the northern sector, commonly associated with RF1 (54.668°N, -6.950°E).

4.3 Site architecture

At each site, radar profiles were divided into radar facies according to Table 1 and Section 4.2 above. Here we describe the architecture of individual esker ridges and outline the processes responsible for their formation.

4.3.1 Site 1

Site 1 is a 1.6 km long, broad, round-crested esker ridge at the northern termination of the single ridge esker system (northern sector). We conducted a 0.9 km, 100 MHz radar survey along a road following the crest of the esker ridge (Fig. 6). The ridge is situated along a forest-covered valley bottom on a slope that dips towards the southwest and is significantly wider than southerly ridges within the system (up to 140 m wide and 16 m high). The esker surface displays minor undulations (<1 m over ~ 90 m).

The architecture of the esker ridge is defined by a semi-continuous bounding surface with varying elevation along the upper part of the radar profile (Fig. 6). Below this bounding surface is a core of RF1

present along the whole esker profile. The chaotic reflections suggest coarser material with a lack of structure, so are interpreted to have formed by rapid deposition during high flow velocities (Burke *et al.,* 2010; Pellicer and Gibson, 2011; Franke *et al.,* 2015; Livingstone *et al.,* 2016). At around 500 m along the profile, side-swipes are observed, likely relating to signal scattering from surface obstacles (Cassidy and Jol, 2009). No lower bounding surface is observed for this unit, but a maximum thickness of 15 m is present at ~ 600 m. Towards the esker surface, the semi-continuous bounding surface defines units of RF4 from 250 m onwards. The concave basin-infills (RF4) vary in size, up to ~ 6 m deep and ~ 80 m wide. At multiple locations the contact with RF4 and underlying reflectors is erosional (Fig. 6). The reflectors observed in these concave infills are less chaotic, which we interpret to have formed as cut-and-fill features, with deposition of finer sediment during waning flow (Sambrook-Smith *et al.,* 2006; Franke *et al.,* 2015; Table 1). Cut-and-fill structures observed in eskers have previously been interpreted to occur when thermomechanical excavation is outweighed by creep closure, leading to increased flow velocities and the erosion of underlying sediments (Perkins *et al.,* 2016).

4.3.2 Site 2

Fig. 7 shows a 0.6 km, 160 MHz radar profile taken along the crest of a 1.9 km long, round-crested ridge, near the southern end of the simple esker system (northern sector). Fig. 8 displays a cross-profile (including a short long-profile section of the crestline), taken from just over halfway along the ridge. The topographic context of the system is largely uniform, with the ridge trending up a reverse bed slope along the valley floor. The ridge morphology varies along its length. Undulations (up to 2 m high) are observed to be associated with esker widening, and the ridge generally becomes smaller towards the north (downflow), terminating in a fan-shaped deposit.

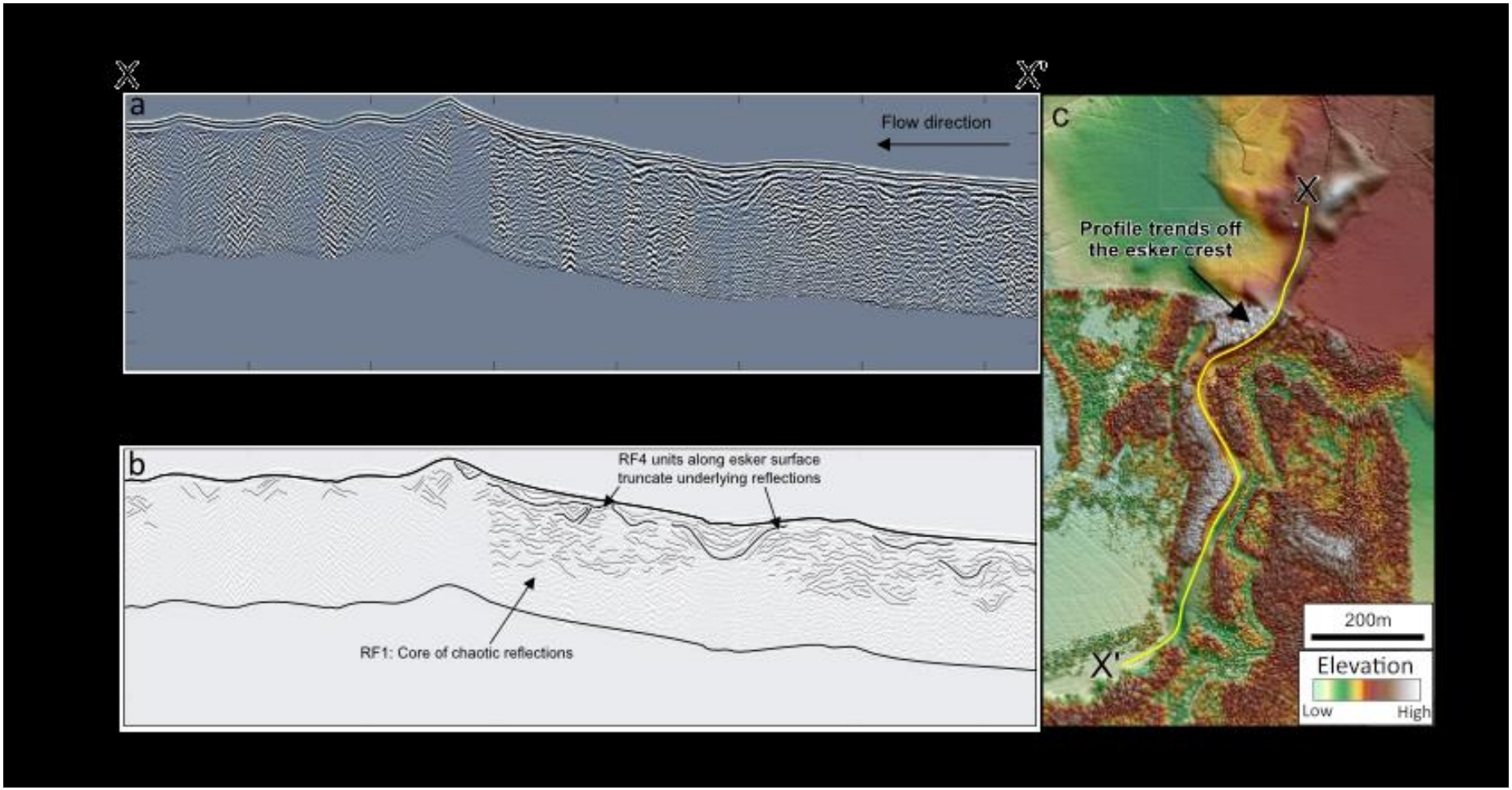

Figure 6. (a)100 MHz long-profile radar survey along the crest of a single ridge esker towards the NE terminus of the County Tyrone Esker, the location of the survey line is presented in Fig. 2. Ice flow direction is indicated by the black arrow. (b) shows an interpreted radar profile derived through the tracing of key reflections. (c) Inset figure showing the detailed esker morphology and the location of radar survey (yellow line).

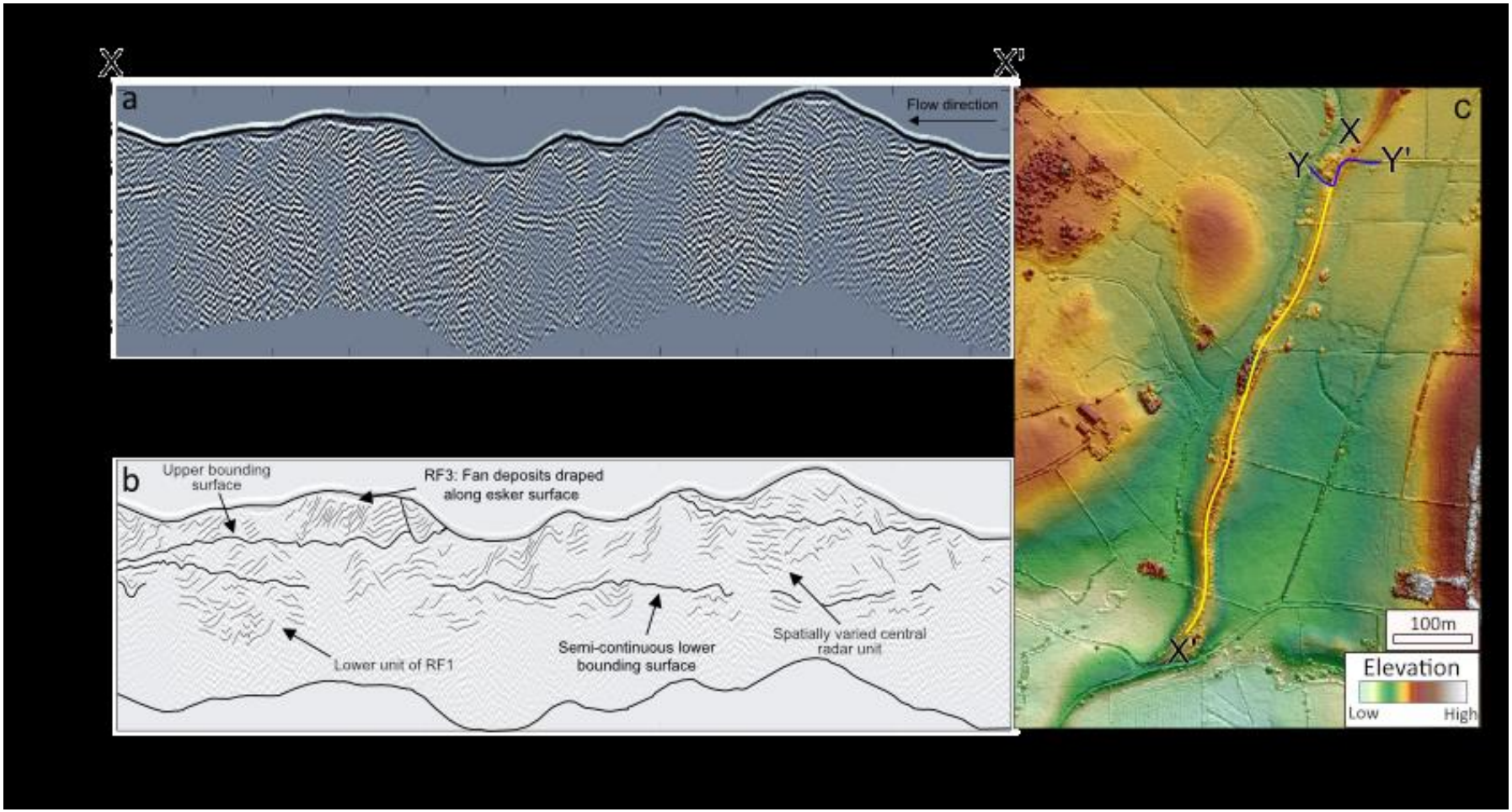

Figure 7. (a) 160 MHz long-profile radar survey along the crest of a single ridge esker near the initiation of the simple system, the location of the survey line is presented in Fig. 2. Ice flow direction is indicated by the black arrow. (b) shows an interpreted radar profile derived through the tracing of key reflections. (c) Inset figure showing the detailed esker morphology and the location of radar survey for figure 7 (yellow line) and the radar survey line for figure 8 (blue line).

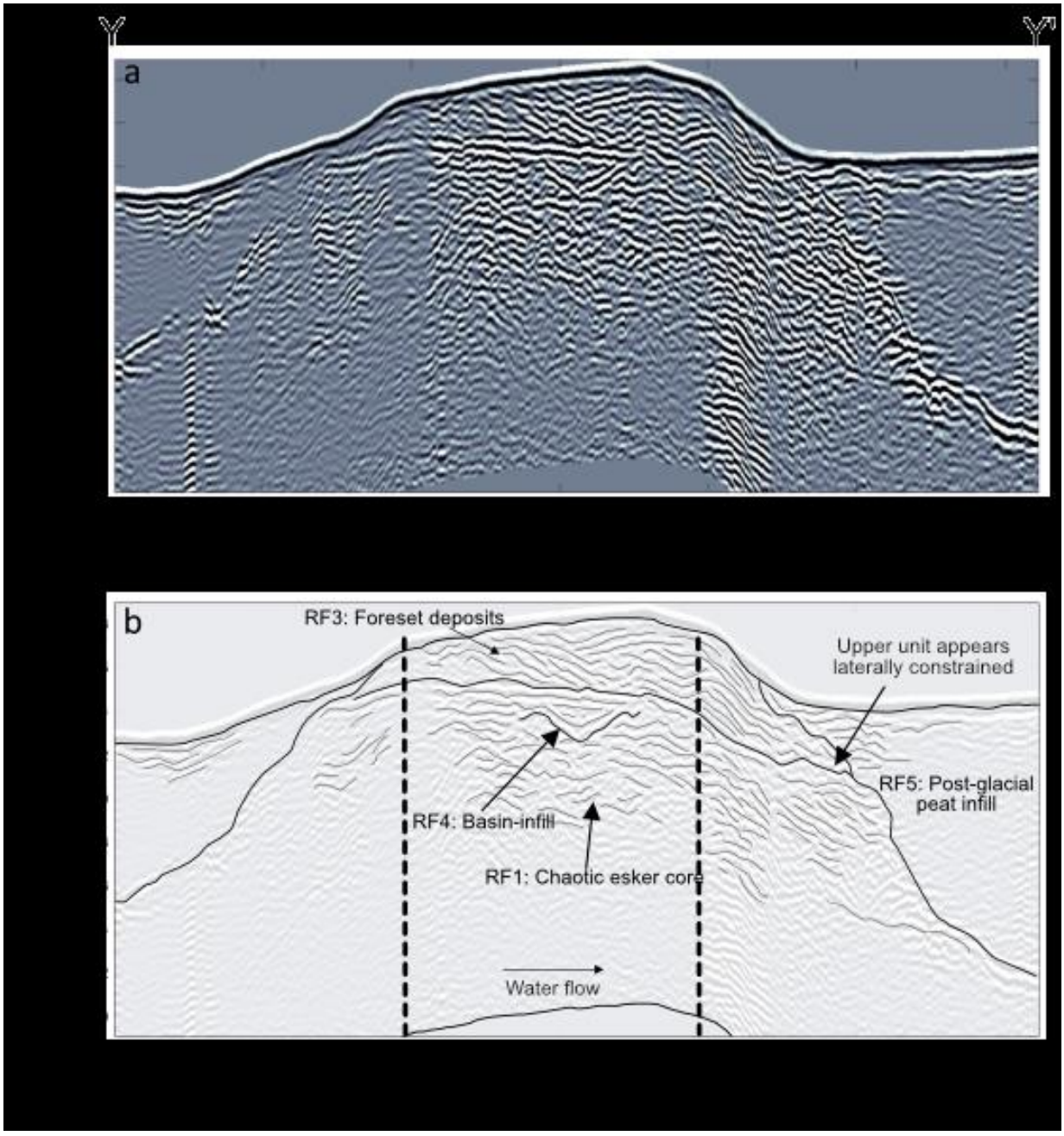

Figure 8. (a) 160 MHz long-profile radar survey along the crest of a single ridge esker near the initiation of the simple system, the location of the survey line is presented in Fig. 2. Ice flow direction is indicated by the black arrow. (b) shows an interpreted radar profile derived through the tracing of key reflections, vertical dashed lines indicate the portion of the radar survey which travelled along the esker ridge. The location of the radar profile is indicated on Fig. 7c by a blue line.

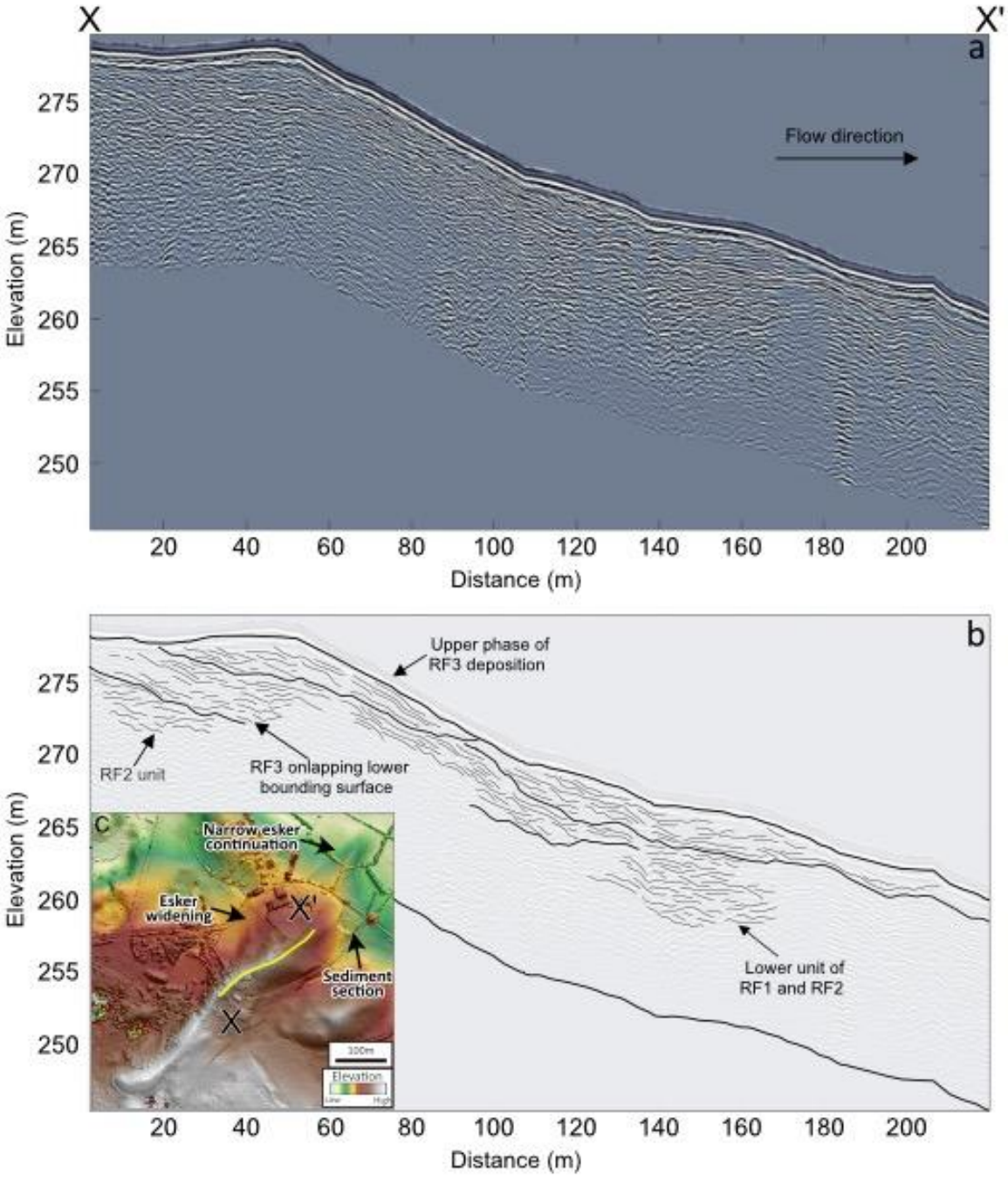

Figure 9. (a) 160 MHz radar profile along the crest of an esker within the complex central sector. The red line indicates the radar survey location and the white dot shows the photograph location in Fig. 5b. Ice flow direction is indicated by the black arrow. (b) shows an interpreted radar profile derived through the tracing of key reflections, vertical dashed lines indicate the portion of the radar survey which travelled along the esker ridge. (c) Inset figure showing the detailed esker morphology and the location of radar survey (yellow line), while the labelled sediment section is photographed in Fig. 5b.

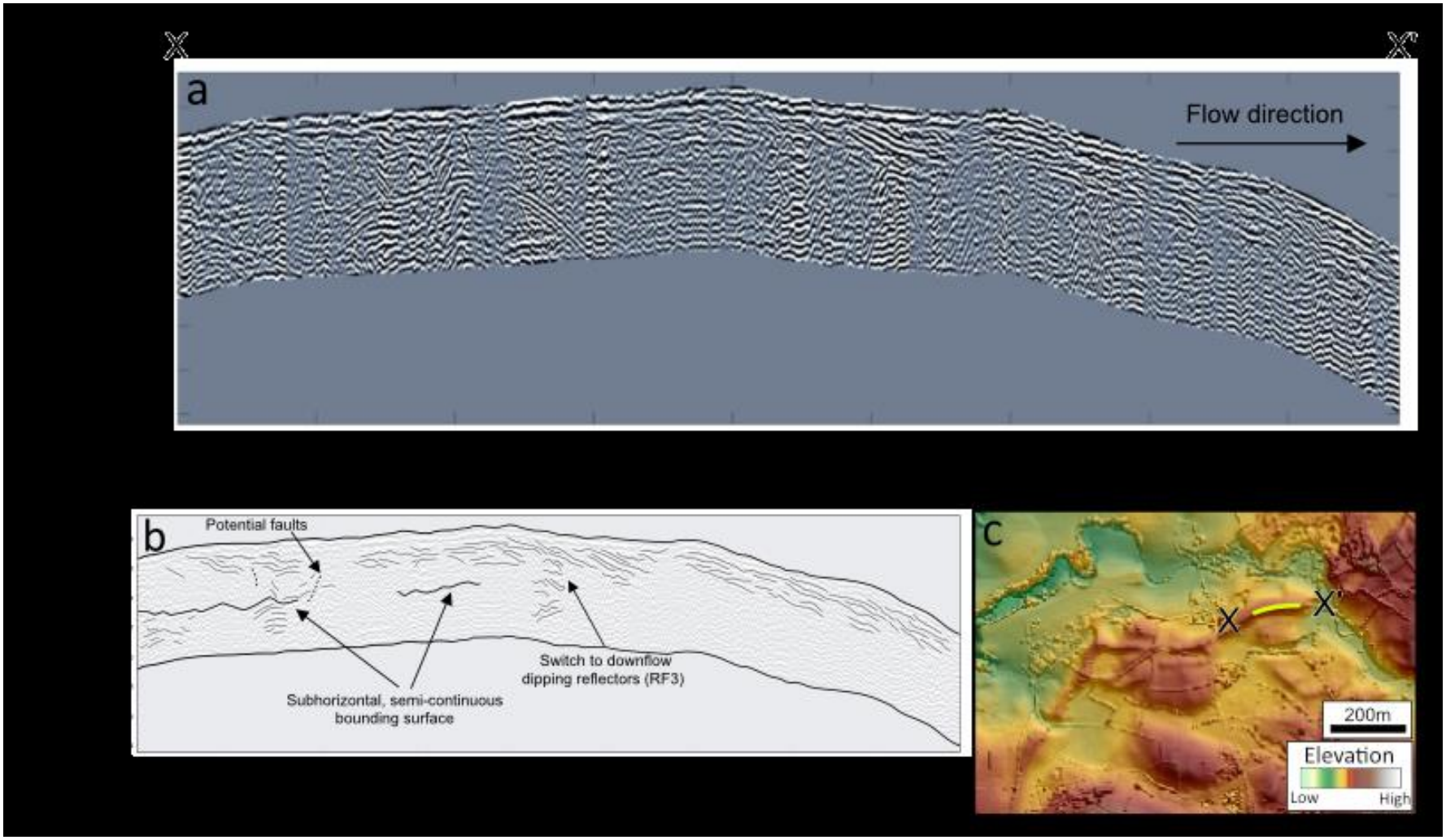

441

442 Figure 10. (a) 160 MHz radar profile along the crest of an esker within the southern sector. Ice flow direction is indicated by the black arrow. (b) shows an
443 interpreted radar profile derived through the tracing of key reflections, vertical dashed lines indicate the portion of the radar survey which travelled along the
444 esker ridge. (c) Inset figure showing the detailed esker morphology and the location of radar survey (yellow line).

Two strong, horizontal bounding reflectors divide the ridge into three architectural units. These bounding surfaces are discordant with the undulating esker surface. The lowest bounding surface is observed at ~224 m elevation, with the underlying unit comprising a core of RF1 (present along the length of the profile). Variations in thickness (~1 - 4 m) are observed, although no clear esker base is identified. Between 0 - 10 m distance, a single unit of RF4 is present, cutting into RF1 with a depth of ~1 m. This lower radar element relates to the initial stages of esker formation, and indicates high flow energy and deposition of coarse material (Pellicer and Gibson, 2011; Livingstone *et al.,* 2016). Above the bounding surface at ~224m elevation, the radar facies of the central unit varies spatially. Chaotic reflections (RF1) dominate the upflow section from 400 – 550 m distance. Moving downflow, these reflections become more continuous and in places exhibit a downflow dip (RF3; ~ 250m distance). Above the upper bounding surface (225 m elevation), a ~2 m thick, tabular unit of RF3 is continuous between 0 – 200 m distance, but absent from 200 – 400 m distance. The presence of RF3 indicates a switch to waning flow conditions in a progradational depositional environment. This unit is draped along the esker crest and does not extend over the esker flanks, coinciding with an increase in esker height, this suggests that deposition was constrained by ice walls (Fig. 8). Foreset-backset macroforms have been associated with dynamic subglacial conduit enlargements during high flow energy conditions (Fiore *et al.,* 2002; Burke *et al.,* 2010). The absence of backset deposits within this esker suggests another mechanism was responsible for the change to progradational deposition.

Between 400 - 500 m distance, another radar element is draped over the esker surface, consisting of subhorizontal to chaotic reflections (RF1 and RF2), coincident with an undulation and widening of the esker ridge. Overall, esker architecture records a transition from high-energy flow during the initial stages, to waning flow conditions where depositional processes reflect local ice tunnel conditions. In cross-profile, up to 8 m of post-glacial peat deposition (RF5) is documented on the esker flanks. This may result in less than 50% of the true esker height being observable at the surface (Jol and Smith, 1991; Pellicer et al., 2012).

4.3.3 Site 3

Fig. 9 presents a 0.2 km, 160 MHz radar profile along the crest of a 0.8 km round-topped esker ridge, within the complex multi-ridge system (central sector). The ridge is situated in an area of steep, hilly topography. At ~300m along the esker morphology develops from a narrow ridge (~50m wide) into a broad, fan-shaped enlargement which is ~130m wide and ~250m long, before the ridge terminates in a narrower section (~50m wide) that is ~200m long in an open topographic basin that drains to the northwest. The radar profile starts on the summit of a hill at the beginning of the enlargement and then follows the esker crest downslope (Fig 9). Three other ridges are located adjacent to the studied esker, terminating in the same basin. A gravel pit is located at the terminus of the ridge, consisting of a series of sand and gravel foreset units which dip to the northeast (Fig. 5b).

Within the lowest radar unit, between 0 – 40 m distance, the sequence is dominated by at least 3 m of coherent horizontal reflections (RF2) indicating vertical accretion of fine material (Burke *et al.,* 2012). Poor radar penetration prevents the identification of the lower bounding surface of this unit. From 120 – 170 m along flow, a unit up to 7 m thick, composed of more discontinuous reflections (RF1 and RF2) represent a lateral transition to coarser material lacking structure, interpreted to be deposited subglacially under higher flow energy (Pellicer and Gibson, 2011; Franke *et al.,* 2015; Livingstone *et al.,* 2016). The upper section of the radar profiles is dominated by units of wedge-shaped units composed of continuous downflow dipping reflectors. From 0 – 140 m, the units of RF3 are onlapping, but 140 m onwards is characterised by a single unit of RF3 along the surface. These upper units likely represent a series of foresets and cross-stratified sands and gravels, deposited during low flow energy conditions in a progradational environment (Franke *et al.,* 2015). We interpret this onlapping sequence of foresets, composed of cross-stratified sands and gravels, as an outwash fan deposited as meltwater exits a subglacial conduit at the ice sheet margin (Winsemann *et al.,* 2007). This is supported by the transition to a broader, fan-shaped morphology of the esker enlargement that suggests this outwash fan may be superimposed on a core of material that was deposited subglacially (Fig. 9).

4.3.4 Site 4

Fig. 10 shows a 0.18 km long, 160 MHz radar profile along part of the crest of a 0.75 km round-crested esker within the complex, multi-ridge to anabranching esker system (southern sector). The esker system is situated in an area of complex, hilly topography. The general esker trend is subparallel to a fault-controlled valley, with ridges situated in and around it (Fig. 5d).

A single bounding surface is semi-continuous along the radar profile, present from 0 – 70 m distance, at an elevation of ~ 233 m (Fig. 10). Below this bounding surface, a ~2 m thick core unit of chaotic reflections (RF1) is present in sections of the radar profile where penetration was deep enough. These chaotic reflections suggest the presence of coarse material deposited under high energy flow conditions (Pellicer and Gibson, 2011; Livingstone *et al.,* 2016). Above the bounding surface, the radar units (~4m thick) comprise of more continuous reflections which either subhorizontal or downflow dipping (RF2 and RF3). This represents an increase in structure as finer material was deposited during waning flow conditions (Franke *et al.,* 2015). The upflow section (0 - 80 m distance) is dominated by RF1 and RF2, while the downflow section (80 m distance onwards) consists of more coherent units of RF3. This transition to fine-grained foresets (RF3) coincides with a change to a downslope trend.

5.0 Discussion

The following section seeks to further our understanding of esker formation based on the sedimentary architecture of a morphologically diverse esker system. First, the broad-scale architecture is considered in order to develop a depositional model of esker formation. Second, local controls on esker formation

514 and morphology are discussed. Finally, we use our findings to reconstruct the ice sheet retreat pattern
515 and retreat rate for the Omagh Basin region.

516 5.1 Esker formation

517 a. A two-phase model of esker deposition

518 The Evishanoran Esker has a broadly homogeneous large-scale sedimentary architecture, despite
519 changes in esker morphology and topographic context (Figs. 6-10). GPR surveys reveal two main
520 phases of esker formation. Initial esker growth involved deposition of coarse gravel or diamict from
521 subglacial hyperconcentrated flows, which may have occurred in a somewhat synchronous manner
522 (Saunderson, 1977; Gorrell and Shaw, 1991; Pellicer and Gibson, 2011). Although, offset ridge
523 relationships and eskers terminating in fans in the northern sector suggest that this deposition likely
524 extended for a maximum of a few kilometres up-ice, rather than tens of kilometres (Fig. 4b). Later
525 stages of esker growth coincide with a transition to well-sorted, fine-grained deposits as flow energy
526 wanes (Franke *et al.*, 2015). Radar facies document a variety of hydrological processes during this final
527 phase of formation (RF2, RF3 and RF4), in contrast to the simple earlier phase dominated by
528 hyperconcentrated flows (RF1).

529 As meltwater approaches the ice sheet margin, subglacial conduits experience reduced creep closure
530 (reaching zero at the ice margin: Rothlisberger, 1972). Despite this, thermomechanical excavation
531 continues to enlarge the subglacial conduit, meaning that the subglacial conduit grows towards the ice
532 sheet margin (Drews *et al.*, 2017). This expansion of the subglacial conduit is expected to cause a
533 progressive reduction in flow energy towards the ice sheet margin (Hewitt and Creyts, 2019). This
534 causes a reduction of the carrying capacity and the deposition of well-sorted, finer material. Therefore,
535 sedimentation rates are highest at the ice sheet margin. This results in an enlargement of the esker profile
536 at or near to former ice margin standstills (Fig. 11a). Additionally, as meltwater exits the subglacial
537 conduit at the ice sheet margin, flow expansion will result in a rapid fall in flow energy and the formation
538 of outwash fans and foreset deposits.

539 Esker size, and the thickness of stratigraphic units, is dependent on the duration of deposition and the
540 rate of deposition. As we described, the deposition rate is likely linked to the proximity of a location to
541 the ice sheet margin, as well as rates of sediment supply. While the duration of deposition will be related
542 to the rate of ice sheet margin retreat. Rapid margin retreat will reduce the time available for deposition,
543 while a standstill will result in enhanced deposition at and near the ice sheet margin. Therefore, we
544 suggest that enlargements in the esker profile can indicate a former ice margin position. Under a stable
545 ice sheet margin position, we would expect a simple esker profile which grows in size towards it's
546 terminus. However, variations in the retreat rate during deglaciation will lead to the superimposition of
547 later esker deposits during time-transgressive esker formation (Fig. 11b). We suggest the observed esker
548 enlargements are a form of esker bead deposited at the ice sheet margin, and superimposed on the core

of subglacially deposited coarser material during a two-phase time-transgressive depositional model (Fig. 7, 9 and 11) (Livingstone *et al.*, 2020).

Enlargements in eskers or outwash fans are commonly observed across the Evishanoran Esker. We suggest these enlargements can be used to reconstruct the relative ice sheet margin retreat rate and former ice margin positions. We favour enlargement formation at the ice sheet margin, over the possibility of formation in an enlargement within the subglacial conduit, as we do not observe a backset-foreset macroform which is diagnostic of this formation (Burke *et al.*, 2015). Caution must be taken when using these to reconstruct the retreat rate, as variations in sediment supply may also influence the development of these enlargements. But, the common co-occurrence of esker enlargements with topographic pinning points (Fig. 4a) or moraines (Fig. 4b) supports an ice marginal origin for esker enlargements.

Morphogenetic relationships have been proposed for eskers on the southern Fraser Plateau, British Colombia (Burke *et al.*, 2015; Perkins *et al.*, 2016), while esker complexity has been related to meltwater flow conditions and sediment supply in Svalbard and Iceland (Storrar *et al.*, 2015, 2020). In central Northern Ireland, the relationship between esker morphology and the depositional processes is less clear. At the local scale, undulations and enlargements of the esker profile appear to relate to a two-phase depositional model during ice sheet retreat. An esker core is formed by synchronous subglacial deposition, while enlargements are formed by the time-transgressive deposition of fine sediment near to the ice sheet margin (Fig. 11).

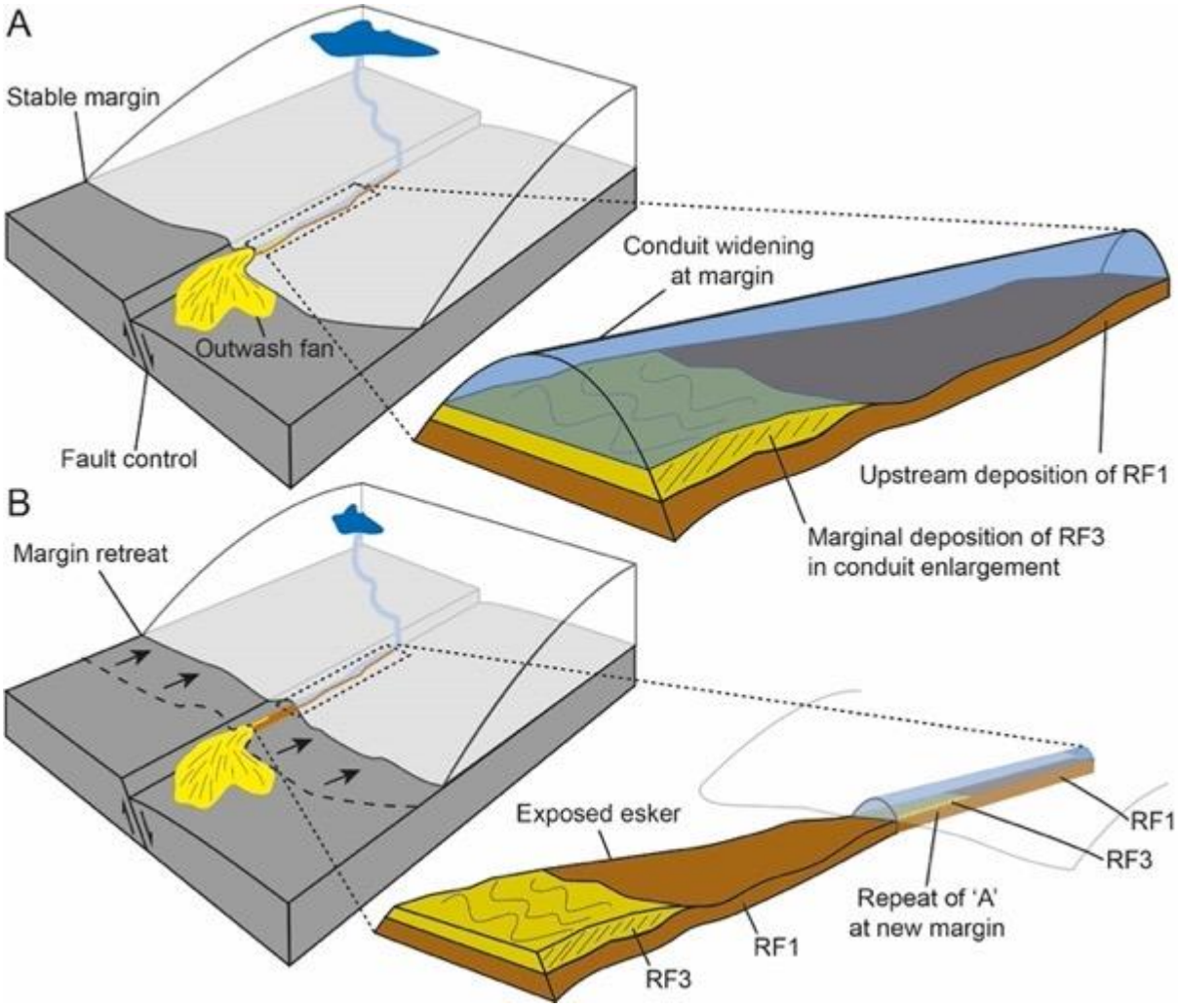

568 Fig. 11. A conceptual model of the two-phase esker deposition. (a) Outwash fans and foresets are
569 deposited at the ice sheet margin due to conduit widening, while coarser material is deposited up-ice in
570 the subglacial conduit. (b) Ice margin retreat leads to the deposition of foresets or outwash fans on top
571 of the core of esker material.

572 b. Local controls

573 The morphology of eskers is influenced by the overall drainage characteristics during formation (Burke
574 *et al.*, 2015; Storrar *et al.*, 2015), as well as local factors (Clark and Walder, 1994; Storrar *et al.*, 2014a;
575 Knight, 2019). Beneath the Laurentide Ice Sheet, complex eskers are more common in areas of greater
576 topographic variability (Storrar *et al.*, 2014a). In the Evishanoran Esker, a similar relationship between
577 complex morphology and topography is observed. At the large-scale, the complex southern and central
578 esker planforms are associated with a topographic context dominated by high variations in relief, while
579 the simpler northern sector is located on the bottom of a broad valley floor. The distribution of eskers
580 in the central sector clearly illustrates this topographic influence, as eskers are deflected around the
581 ~100m hill (Fig. 4c). We propose that esker complexity in central Northern Ireland is largely controlled
582 by the topographic variability. Undulating topography may cause the subglacial conduit to fragment
583 around obstacles or migrate as ice thinned (Wright *et al.*, 2008; Storrar *et al.*, 2014).

The complexity of esker systems in areas of high topographic variability reflects a combination of spatial and temporal changes in the subglacial drainage network. Within the central sector of the Evishanoran Esker, the cross-cutting esker patterns suggest that the drainage system evolved over time to create the complex esker network as the drainage pathways migrated during deglaciation (Fig. 4c). In contrast, the anabranching nature of the southern sector, with no cross-cutting relationships may instead represent a drainage network which is fragmented by the complex topography (Fig. 4d). This is supported by the association with a series of meltwater channels cut into, and ascending, the hill to the south of this sector (Fig. 2b), which may have been active at similar times. Pressurised meltwater eroded the meltwater channels on the southern slopes of the hill. Reductions in pressure on the downslope trend then led to the deposition of the esker system (Livingstone et al., 2016). It is also possible that increased deposition on the downslope trend may have led to channel clogging and avulsion (Storrar *et al.,* 2015).

Substrate characteristics have been hypothesised to influence the formation and distribution of eskers. Eskers are more common on more resistant bedrock (Clark and Walder, 1994), while esker morphology in north-central Ireland is controlled by a variety of substrate factors, including the influence of pre-existing glacial features (Knight, 2019). The transition from sandstone and limestone in the south to the crystalline granites in the north does not appear to influence esker distribution in the region south of the Sperrin Mountains. However, a high level of spatial correspondence between eskers and geological faults is observed (Fig. 2). This correspondence includes eskers in the southern sector running sub-parallel to a large fault-controlled valley, and pronounced changes in the orientation of eskers to trend along faults (Fig. 2). Enhanced groundwater flow along zones of higher transmissivity (e.g. faults) may influence the distribution of the subglacial drainage system (Boulton *et al.,* 2007a; 2007b; 2009). In central Northern Ireland, this relationship appears to strongly control the subglacial drainage network.

The morphometry of eskers may relate to a combination of sediment and meltwater supply (Shreve, 1985; Storrar *et al.,* 2015), but caution must be taken when using solely geomorphological observations of eskers to investigate the hydrological system of a palaeo-ice sheet. Radar surveys revealed substantial post-glacial peat infilling around eskers, reducing the relative relief of eskers in the northern sector. The relative relief of one esker is 5 m, but with up to 6 m of esker deposits hidden below the surface (Fig. 8). Extensive peat deposits have been documented in the Irish Midlands, up to 5.5 m thick (Pellicer and Gibson, 2011; Pellicer *et al.,* 2012), which must be taken into consideration when using esker dimensions to gain an insight into glacial history.

5.2 Implications for deglaciation of Northern Ireland

Three main ice dispersal centres operated during the deglaciation of the north of Ireland. This includes an upland ice dispersal centre in the Donegal Mountains, and lowland ice domes in the Lough Neagh and Omagh basins, which have been well documented in previous literature (Knight, 1997; Knight and McCabe, 1997; McCarron, 2013). Across this region, meltwater landforms and small moraines record

the final retreat pattern of the Irish Ice Sheet. Here we describe the broader retreat patterns of the Irish Ice Sheet, before using the Evishanoran Esker to describe the retreat rate of the Omagh Basin ice.

These ice domes were coalescent at the start of deglaciation, indicated by subglacial bedform patterns (Fig. 2a), but became isolated ice domes followed ice sheet thinning and saddle collapse. Eskers oriented radially around the Lough Neagh basin record the final retreat pattern inwards. Lough Neagh ice separated from the Lough Erne/Omagh Basin ice dome along an approximately N-S axis located to the south of the eastern Sperrin Mountains (Fig. 2a). In the west, the Lough Erne ice dome separated from ice sourced from the Donegal and Sligo Mountains sometime between 15-16ka, according to the isochrons of Wilson *et al.* (2019). Lateral meltwater channels record the downwasting of ice flowing from Sligo and Donegal into the Lough Erne Basin, recording when summits became ice-free and the separation of these ice dispersal centres. The position of these channels suggests Donegal ice flowed into the Lough Erne Basin, indicating that Donegal ice persisted long enough to flow into a mostly deglaciated Lough Erne Basin (Fig. 2b). This is consistent with dating evidence that suggests that the Donegal Mountains held the final remnants of the British-Irish Ice Sheet (Wilson *et al.*, 2019).

The relative retreat rate and former ice margin standstills can be identified from the morphology of the Evishanoran Esker and associated landforms. The initial southwards ice margin retreat from the Sperrin Mountains was quite slow across the northern esker sector. We identify at least four former ice margin standstills over the 9.3 km this sector spans, from evidence of five small moraines, two esker enlargements, three outwash fan deposits and sedimentological information (Fig. 2b,c). These former standstill locations are mostly located at topographic pinning points. The retreat rate was more rapid across the central sector. A single moraine and outwash fan at the northern end of this sector suggest only one standstill, due to their close proximity, across the 7.4 km sector length. The retreat rate across the southern sector may have slowed slightly, as the retreat direction became oriented towards the SW. Geomorphological evidence suggests one or two possible standstills over a distance of 6.5 km. A small moraine at the north-eastern side of the sector suggests a standstill at the start of esker formation in this sector, where a hill (~150m relative relief) may have acted as a pinning point. A small enlargement associated with foreset deposits may have formed under a short-lived standstill in the centre of this sector (Fig. 10). However, the retreat was likely more rapid than in the northern sector due to the relative lack of geomorphological evidence.

6.0 Conclusions

The Evishanoran Esker was deposited time-transgressively in a subglacial, closed conduit or at the ice sheet margin and records the final stages of ice retreat in this region from the Sperrin Mountains to the south. Esker distribution is a result of the dynamic evolution of the subglacial hydrological system, and does not record an extensive drainage network. Based on our observations, we present a series of key points regarding the deglacial history and broader implications for esker formation:

1. Deposition of the Evishanoran Esker occurred in two main flow phases. An initial phase of semi-synchronous, subglacial deposition formed the esker core. A second phase of time-transgressive deposition near the ice sheet margin. This occurs as the subglacial conduit enlarges due to reduced creep closure, causing an increase in deposition of fine material and foresets. Esker enlargements occur where these time-transgressive deposits are observed, and can indicate former ice margin positions.
2. The internal architecture of eskers is broadly homogenous across all sectors, suggesting that hydrological conditions are largely comparable across the sectors. Variations in esker morphology cannot solely attributed to variations in drainage characteristics. Instead we suggest local topographic conditions influence esker complexity.
3. Using evidence for former ice margin standstills we reconstruct the variations in the retreat rate across the Evishanoran Esker. Ice margin retreat across the northern sector was slow, with retreat rate increasing during margin retreat across the central and southern sectors.
4. Geologic and topographic settings control esker distribution and formation. The close association between the orientation and distribution of eskers and faults suggest that underlying geological structural weaknesses act as a zone of high meltwater transmissivity. The reconstruction of ice dynamics from meltwater features must also consider the influence of local factors on distribution.
5. Post-depositional processes can have a significant influence on esker geomorphology. Post-glacial fluvial erosion has previously been invoked to explain the fragmentation of some esker systems. We identify significant post-glacial peat infilling which masks esker dimensions and poses a problem for esker studies that rely solely on remote sensing morphometric analysis.

Acknowledgements:

We thank Mike Langton of GuideLineGeo (MALA) for the loan of radar equipment and advice. Digital resources were made available under MOU205, courtesy of Land and Property Services, Northern Ireland, supplied to Queen's University, Belfast. This study would also not be possible without the generous access to land granted by multiple landowners in Northern Ireland.

References

Alley, R.B., Blankenship, D.D., Bentley, C.R. and Rooney, S.T. (1986) Deformation of till beneath ice stream B, West Antarctica. Nature 322, 57-59.

Aylsworth, J.M. and Shilts, W.W. (1989) Bedforms of the Keewatin ice sheet, Canada. *Sedimentary Geology*, *62*(2-4): 407-428

Banerjee, I. and McDonald, B.C. (1975) Nature of esker sedimentation, in Jopling, A. V., and McDonald, B. C., eds., Glaciofluvial and glaciolacustrine sedimentation: Society of Economic Paleontologists and Mineralogists Special Publication No. 23: 132-154.

689 Bartholomew, I., Nienow, P., Mair, D., Hubbard, A., King, M.A. and Sole, A. (2010). Seasonal
690 evolution of subglacial drainage and acceleration in a Greenland outlet glacier. Nature
691 Geoscience, 3(6), 408-411.

692 Bell, R.E., Studinger, M., Shuman, C.A., Fahnestock, M.A. and Joughin, I. (2007). Large subglacial
693 lakes in East Antarctica at the onset of fast-flowing ice streams. Nature, 445(7130), 904-
694 907.

695 Boulton, G.S., Lunn, R., Vidstrand, P. and Zatsepin, S., (2007a) Subglacial drainage by
696 groundwater-channel coupling, and the origin of esker systems: part 1—glaciological
697 observations. *Quaternary Science Reviews*, *26*(7-8), 1067-1090

698 Boulton, G.S., Lunn, R., Vidstrand, P. and Zatsepin, S. (2007b) Subglacial drainage by
699 groundwater–channel coupling, and the origin of esker systems: part II—theory and
700 simulation of a modern system. *Quaternary Science Reviews*, *26*(7-8), 1091-1105

701 Boulton, G.S., Hagdorn, M., Maillot, P.B. and Zatsepin, S. (2009) Drainage beneath ice sheets:
702 groundwater–channel coupling, and the origin of esker systems from former ice
703 sheets. *Quaternary Science Reviews*, *28*(7-8), 621-638

704 Bradwell, T., Stoker, M.S., Golledge, N.R., Wilson, C.K., Merritt, J.W., Long, D., Everest, J.D.,
705 Hestvik, O.B., Stevenson, A.G., Hubbard, A.L. and Finlayson, A.G. (2008) The northern
706 sector of the last British Ice Sheet: maximum extent and demise. *Earth-Science*
707 *Reviews*, *88*(3-4): 207-226

708 Brennand, T. A. (1994). Macroforms, large bedforms and rhythmic sedimentary sequences in
709 subglacial eskers, south-central Ontario: implications for esker genesis and meltwater
710 regime. *Sedimentary Geology*, *91*(1–4), 9–55. https://doi.org/10.1016/0037-0738(94)90122-
711 8

712 Brennand, T.A. (2000) Deglacial meltwater drainage and glaciodynamics: inferences from
713 Laurentide eskers, Canada. *Geomorphology*, *32*(3-4): 263-293

714 Budd, W.F., Keage, P.L. and Blundy, N.A (1979). Empirical studies of ice sliding. Journal of
715 Glaciology, 23, 157-170.

716 Burke, M. J., Brennand, T. A., & Sjogren, D. B. (2015). The role of sediment supply in esker
717 formation and ice tunnel evolution. *Quaternary Science Reviews*, *115*, 50–77.
718 https://doi.org/10.1016/j.quascirev.2015.02.017

719 Burke, M. J., Woodward, J., Russell, A. J., Fleisher, P. J., & Bailey, P. K. (2008). Controls on the
720 sedimentary architecture of a single event englacial esker: Skeiðarárjökull, Iceland.
721 *Quaternary Science Reviews*, *27*(19–20): 1829–1847.
722 https://doi.org/10.1016/j.quascirev.2008.06.012

723 Burke, M. J., Woodward, J., Russell, A. J., Fleisher, P. J., & Bailey, P. K. (2010). The sedimentary
724 architecture of outburst flood eskers: A comparison of ground-penetrating radar data from
725 Bering Glacier, Alaska and Skeiarárjökull, Iceland. *Bulletin of the Geological Society of*
726 *America*, *122*(9–10): 1637–1645. https://doi.org/10.1130/B30008.1

727 Burke, M.J., Brennand, T.A. and Perkins, A.J. (2012) Transient subglacial hydrology of a thin ice
728 sheet: insights from the Chasm esker, British Columbia, Canada. *Quaternary Science*
729 *Reviews*, *58*: 30-55.

730 Cassidy, N.J. and Jol, H.M. (2009) Ground penetrating radar data processing, modelling and
731 analysis. *Ground penetrating radar: theory and applications*: 141-176

732 Charlesworth, J.K. (1921). The glacial geology of the north-west of lreland. *Proceedings of the*
733 *Royal lrish Academy*, 36b: 174-314

734 Charlesworth, J.K. (1921) The Evishnoran "Esker", Tyrone. *Geological Magazine*, 63(5), 223-225.
735 doi:10.1017/S0016756800084156

736 Chiverrell, R.C., Thomas, G.S.P., Burke, M., Medialdea, A., Smedley, R., Bateman, M., Clark, C.,
737 Duller, G.A., Fabel, D., Jenkins, G. and Ou, X., 2020. The evolution of the terrestrial-
738 terminating Irish Sea glacier during the last glaciation. Journal of Quaternary Science

739 Clark, C.D. and Meehan, R.T. (2001) Subglacial bedform geomorphology of the Irish Ice Sheet
740 reveals major configuration changes during growth and decay. *Journal of Quaternary*
741 *Science: Published for the Quaternary Research Association*, *16*(5): 483-496

742 Clark, C.D., Ely, J.C., Greenwood, S.L., Hughes, A.L., Meehan, R., Barr, I.D., Bateman, M.D.,
743 Bradwell, T., Doole, J., Evans, D.J. and Jordan, C.J. (2018) BRITICE Glacial Map, version
744 2: a map and GIS database of glacial landforms of the last British–Irish Ice
745 Sheet. *Boreas*, *47*(1): 11

746 Clark, C.D., Hughes, A.L., Greenwood, S.L., Jordan, C. and Sejrup, H.P. (2012) Pattern and timing
747 of retreat of the last British-Irish Ice Sheet. *Quaternary Science Reviews*, *44*: 112-146

748 Clark, P. U., & Walder, J. S. (1994). Subglacial drainage, eskers, and deforming beds beneath the
749 Laurentide and Eurasian ice sheets. *Geological Society of America Bulletin*, *106*(2), 304–
750 314. https://doi.org/10.1130/0016-7606(1994)106<0304:SDEADB>2.3.CO;2

751 Cofaigh, C.Ó., Weilbach, K., Lloyd, J.M., Benetti, S., Callard, S.L., Purcell, C., Chiverrell, R.C.,
752 Dunlop, P., Saher, M., Livingstone, S.J. and Van Landeghem, K.J. (2019) Early deglaciation
753 of the British-Irish Ice Sheet on the Atlantic shelf northwest of Ireland driven by
754 glacioisostatic depression and high relative sea level. *Quaternary Science Reviews*, *208*: 76-
755 96.

756 Colhoun, A. (1971) The glacial stratigraphy of the Sperrin Mountains and its relation to the glacial
757 stratigraphy of north-west Ireland. Proceedings of the Royal Irish Academy 71B: 37–52

758 Colhoun, E.A. (1970). On the nature of the glaciations and final deglaciation of the Sperrin
759 Mountains and adjacent areas in the north of Ireland. *Irish Geography*, 6(2), 162-185.

760 Cummings, D.I., Kjarsgaard, B.A., Russell, H.A. and Sharpe, D.R. (2011) Eskers as mineral
761 exploration tools. *Earth-science reviews*, *109*(1-2): 32-43

762 Davison, B.J., Sole, A.J., Livingstone, S.J., Cowton, T.R. and Nienow, P.W. (2019) The influence of
763 hydrology on the dynamics of land-terminating sectors of the Greenland Ice Sheet. *Frontiers*
764 *in Earth Science, 7*.

765 Delaney, C. (2001a) Esker formation and the nature of deglaciation: the Ballymahon esker, Central
766 Ireland. *North West Geography, 1*(2): 23-33

767 Delaney, C. (2001b) Morphology and sedimentology of the Rooskagh esker, Co. Roscommon. *Irish*
768 *Journal of Earth Sciences*: 5-22

769 Delaney, C. (2002) Sedimentology of a glaciofluvial landsystem, Lough Ree area, Central Ireland:
770 implications for ice margin characteristics during Devensian deglaciation. *Sedimentary*
771 *Geology*, *149*(1-3): 111-126

772 Delaney, C.A., McCarron, S. and Davis, S. (2018). Irish Ice Sheet dynamics during deglaciation of
773 the central Irish Midlands: Evidence of ice streaming and surging from airborne LiDAR.
774 *Geomorphology,* 306, 235-253.

775 Drews, R., Pattyn, F., Hewitt, I.J., Ng, F.S.L., Berger, S., Matsuoka, K., Helm, V., Bergeot, N.,
776 Favier, L. and Neckel, N. (2017) Actively evolving subglacial conduits and eskers initiate
777 ice shelf channels at an Antarctic grounding line. *Nature communications, 8*: 15228

778 Dyke, A. and Prest, V. (1987) Late Wisconsinan and Holocene history of the Laurentide ice
779 sheet. *Géographie physique et Quaternaire*, *41*(2): 237-263.

780 Evans, D. J. A., & Benn, D. I. (2004) A practical guide to the study of glacial sediments. Edward
781 Arnold, London.

782 Fiore, J., Pugin, A. and Beres, M. (2002) Sedimentological and GPR studies of subglacial deposits
783 in the Joux Valley (Vaud, Switzerland): backset accretion in an esker followed by an erosive
784 jökulhlaup. *Géographie physique et Quaternaire*, *56*(1): 19-32

785 Fitzsimons, S.J. (1991) Supraglacial eskers in Antarctica. *Geomorphology*, *4*(3-4): 293-299

786 Flint, R.F. (1930) The Origin of the Irish" Eskers". *Geographical Review, 20*(4): 615-630

787 Franke, D., Hornung, J. and Hinderer, M. (2015) A combined study of radar facies, lithofacies and
788 three-dimensional architecture of an alpine alluvial fan (Illgraben fan,
789 Switzerland). *Sedimentology*, *62*(1): 57-86

790 Gawthorpe, R.L., Collier, R.L., Alexander, J., Bridge, J.S. and Leeder, M.R. (1993) Ground
791 penetrating radar: application to sandbody geometry and heterogeneity studies. *Geological*
792 *Society, London, Special Publications*, *73*(1): 421-432

793 Geological Survey Northern Ireland (2016) Digital Geological Map of Northern Ireland – 10k. 10k
794 geology reproduced with the permission of the Geological Survey of Northern Ireland.
795 Crown Copyright 2018.

796 Gorrell, G. and Shaw, J. (1991) Deposition in an esker, bead and fan complex, Lanark, Ontario,
797 Canada. *Sedimentary Geology*, *72*(3-4): 285-314

798 Greenwood, S.L., Clark, C.D. and Hughes, A.L., 2007. Formalising an inversion methodology for
799 reconstructing ice-sheet retreat patterns from meltwater channels: application to the British
800 Ice Sheet. *Journal of Quaternary Science: Published for the Quaternary Research*
801 *Association*, *22*(6), pp.637-645

802 Greenwood, S. L., & Clark, C. D. (2009a). Reconstructing the last Irish Ice Sheet 1: changing flow
803 geometries and ice flow dynamics deciphered from the glacial landform record. *Quaternary*
804 *Science Reviews*, *28*(27–28), 3085–3100. https://doi.org/10.1016/j.quascirev.2009.09.008

805 Greenwood, S. L., & Clark, C. D. (2009b). Reconstructing the last Irish Ice Sheet 2: a
806 geomorphologically-driven model of ice sheet growth, retreat and dynamics. *Quaternary*
807 *Science Reviews*, *28*(27–28), 3101–3123. https://doi.org/10.1016/j.quascirev.2009.09.014

808 Greenwood, S.L., Clason, C.C., Helanow, C. and Margold, M. (2016) Theoretical, contemporary
809 observational and palaeo-perspectives on ice sheet hydrology: processes and
810 products. *Earth-Science Reviews*, *155*: 1-27

811 Gregory, J.W. (1912) The relations of kames and eskers. *The Geographical Journal*, *40*(2): 169-175.

812 Gregory, J.W. (1921) IV.—The Irish eskers. *Phil. Trans. R. Soc. Lond. B*, *210*(372-381): 115-151.

813 Gregory, J.W. (1925) The Evishanoran Esker, 1 Tyrone. *Geological Magazine*, *62*(10): 451-458.

814 Gregory, J.W. (1926) The Evishnoran "Esker". *Geological Magazine*, 62(7): 336-336.

815 doi:10.1017/S0016756800084557

816 Gustavson, T.C. and Boothroyd, J.C. (1987) A depositional model for outwash, sediment sources,
817 and hydrologic characteristics, Malaspina Glacier, Alaska: A modern analog of the
818 southeastern margin of the Laurentide Ice Sheet. *Geological Society of America*
819 *Bulletin*, *99*(2): 187-200.

820 Hebrand, M. and Åmark, M. (1989) Esker formation and glacier dynamics in eastern Skane and
821 adjacent areas, southern Sweden. *Boreas*, *18*(1): 67-81.

822 Hewitt, I.J. and Creyts, T.T., 2019. A model for the formation of eskers. *Geophysical Research*
823 *Letters*, *46*(12), pp.6673-6680.

824 Hinch, J. (1921) The eskers of Ireland. *The Irish Naturalist*, *30*(12): 137-142

825 Hubbard, B. & Nienow, P. (1997) Alpine subglacial hydrology. *Quaternary Science Reviews*, 16,
826 939-955.

827 Iken, A., Bindschadler, R.A. (1986). Combined measurements of subglacial water pressure and
828 surface velocity of Findelengletscher, Switzerland: conclusions about drainage system and
829 sliding mechanism. Journal of Glaciology, 32(110), 101-119.

830 Jol, H.M. and Smith, D.G. (1991) Ground penetrating radar of northern lacustrine deltas. *Canadian*
831 *Journal of Earth Sciences*, *28*(12): 1939-1947

Knight, J. (1997). Morphological and morphometric analysis of drumlin bedforms in the Omagh Basin, north central Ireland. *Geografiska Annaler*, 79A: 255-266.

Knight, J. (1999). Geological evidence for neotectonic activity during deglaciation of the southern Sperrin Mountains, Northern Ireland. *Journal of Quaternary Science*, 14(1), 45-57.

Knight, J. (2003). Bedform patterns, subglacial meltwater events, and Late Devensian ice sheet dynamics in north-central Ireland. *Global and Planetary Change*, *35*(3–4), 237–253.

Knight, J. (2006) Geomorphic evidence for active and inactive phases of Late Devensian ice in north-central Ireland. *Geomorphology*, *75*(1-2): 4-19

Knight, J. (2019) The geomorphology and sedimentology of eskers in north-Central Ireland. *Sedimentary Geology*, 382: 1-24.

Knight, J. and McCabe, A.M. (1997) Identification and significance of ice-flow-transverse subglacial ridges (Rogen moraines) in northern central Ireland. *Journal of Quaternary Science*, *12*(6): 519-524

Knight, J., Coxon, P., McCabe, A.M. and McCarron, S.G. (2004) Pleistocene glaciations in Ireland. In *Developments in Quaternary Sciences* (Vol. 2, pp. 183-191). Elsevier

Knight, J., Coxon, P., McCabe, A.M. and McCarron, S.G. (2004) Pleistocene glaciations in Ireland. In *Developments in Quaternary Sciences* (Vol. 2, pp. 183-191). Elsevier.

Livingstone, S. J., Utting, D. J., Ruffell, A., Clark, C. D., Pawley, S., Atkinson, N., & Fowler, A. C. (2016). Discovery of relict subglacial lakes and their geometry and mechanism of drainage. *Nature Communications*, *7*. https://doi.org/10.1038/ncomms11767

Livingstone, S.J., Storrar, R.D., Hillier, J.K., Stokes, C.R., Clark, C.D. and Tarasov, L. (2015) An ice-sheet scale comparison of eskers with modelled subglacial drainage routes. *Geomorphology*, *246*: 104-112

Livingstone, S.J., Lewington, E.L., Clark, C.D., Storrar, R.D., Sole, A.J., McMartin, I., Dewald, N. and Ng, F., 2020. A quasi-annual record of time-transgressive esker formation: implications for ice-sheet reconstruction and subglacial hydrology. *The Cryosphere*, *14*(6), pp.1989-2004

Mäkinen, J. (2003) Time-transgressive deposits of repeated depositional sequences within interlobate glaciofluvial (esker) sediments in Köyliö, SW Finland. *Sedimentology*, *50*(2): 327-360

Margold, M., Jansson, K.N., Kleman, J., Stroeven, A.P. and Clague, J.J. (2013) Retreat pattern of the Cordilleran Ice Sheet in central British Columbia at the end of the last glaciation reconstructed from glacial meltwater landforms. *Boreas*, *42*(4): 830-847

McCabe, A.M. (2008) *Glacial geology and geomorphology: the landscapes of Ireland*. Dunedin Academic Press Ltd.

McCarron, S., 2014. Deglaciation of the Dungiven Basin, North-West Ireland. *Irish Journal of Earth Sciences*, *31*, pp.43-71

868 Miall, A.D. (1985) Architectural-element analysis: a new method of facies analysis applied to fluvial
869 deposits. *Earth Sci. Rev.*, 22, 261–308

870 Neal, A. (2004) Ground-penetrating radar and its use in sedimentology: principles, problems and
871 progress. *Earth-science reviews*, *66*(3-4): 261-330

872 Ó Cofaigh, C., Evans, D.J.A. (2007) Radiocarbon constraints on the age of the maximum advance of
873 the British-Irish Ice Sheet in the Celtic Sea. Quaternary Science Reviews 26 (9–10), 1197–
874 1203

875 Pellicer, X. M., & Gibson, P. (2011). Electrical resistivity and Ground Penetrating Radar for the
876 characterisation of the internal architecture of Quaternary sediments in the Midlands of
877 Ireland. *Journal of Applied Geophysics*, *75*(4), 638–647.
878 https://doi.org/10.1016/j.jappgeo.2011.09.019

879 Pellicer, X. M., Warren, W. P., Gibson, P., & Linares, R. (2012). Construction of an evolutionary
880 deglaciation model for the Irish midlands based on the integration of morphostratigraphic
881 and geophysical data analyses. *Journal of Quaternary Science*, *27*(8), 807–818.
882 https://doi.org/10.1002/jqs.2570

883 Perkins, A. J., Brennand, T. A., & Burke, M. J. (2016). Towards a morphogenetic classification of
884 eskers: Implications for modelling ice sheet hydrology. *Quaternary Science Reviews*, *134*,
885 19–38. https://doi.org/10.1016/j.quascirev.2015.12.015

886 Perkins, A.J., Brennand, T.A. and Burke, M.J. (2013) Genesis of an esker-like ridge over the
887 southern Fraser Plateau, British Columbia: Implications for paleo-ice sheet reconstruction
888 based on geomorphic inversion. *Geomorphology*, *190*:27-39

889 Price, R.J. (1969) Moraines, sandar, kames and eskers near Breidamerkurjökull,
890 Iceland. *Transactions of the Institute of British Geographers*: 17-43

891 Roberts, M.C., Niller, H.P. and Helmstetter, N. (2003) Sedimentary architecture and radar facies of a
892 fan delta, Cypress Creek, West Vancouver, British Columbia. *Geological Society, London,*
893 *Special Publications*, *211*(1): 111-126

894 Röthlisberger, H. (1972) Water pressure in intra-and subglacial channels. *Journal of*
895 *Glaciology*, *11*(62): 177-203

896 Russell, A.J., Knudsen, O., Fay, H., Marren, P.M., Heinz, J. and Tronicke, J. (2001) Morphology
897 and sedimentology of a giant supraglacial, ice-walled, jökulhlaup channel, Skeiðarárjökull,
898 Iceland: implications for esker genesis. *Global and Planetary Change*, *28*(1-4): 193-216

899 Rust, B.R. (1977) Mass flow deposits in a Quaternary succession near Ottawa, Canada: diagnostic
900 criteria for subaqueous outwash. *Canadian Journal of Earth Science*, 14: 175-184

901 Sambrook-Smith, G.H., Ashworth, P.J., Best, J.L., Woodward, J. and Simpson, C.J. (2006) The
902 sedimentology and alluvial architecture of the sandy braided South Saskatchewan River,
903 Canada. *Sedimentology*, *53*(2): 413-434

Saunderson, H.C. (1977) The sliding bed facies in esker sands and gravels: a criterion for full-pipe (tunnel) flow? *Sedimentology*, *24*(5):623-638

Schoof, C. (2010) Ice-sheet acceleration driven by melt supply variability. *Nature*, *468*(7325): 803

Shreve, R. L. (1985). Esker characteristics in terms of glacier physics, Katahdin esker system, Maine. *Geological Society of America Bulletin*, *96*(5), 639–646. https://doi.org/10.1130/0016-7606(1985)96<639:ECITOG>2.0.CO;2

Smith, M. J. & Clark, C. D. (2005) Methods for the visualization of digital elevation models for landform mapping. *Earth Surface Processes and Landforms*, 30, 885-900

Smith, M.J. and Clark, C.D. (2005) Methods for the visualization of digital elevation models for landform mapping. *Earth Surface Processes and Landforms*, *30*(7): 885-900

Smith, M.J. and Knight, J. (2011) Palaeoglaciology of the last Irish Ice Sheet reconstructed from striae evidence. *Quaternary Science Reviews,* 30(1-2): 147-160

Sollas, W.J. (1896) A map to show the Distribution of Eskers in Ireland. *Sci. Trans. R. Dublin Soc,* 2(5): 785-822.

Stearns, L.A., Smith, B.E. and Hamilton, G.S. (2008). Increased flow speed on a large East Antarctic outlet glacier caused by subglacial floods. Nature Geoscience, 1(12), 827-831.

Storrar, R.D., Ewertowski, M., Tomczyk, A.M., Barr, I.D., Livingstone, S.J., Ruffell, A., Stoker, B.J. and Evans, D.J. (2020) Equifinality and preservation potential of complex eskers. *Boreas*, 49(1), 211-231.

Storrar, R. D., Evans, D. J. A., Stokes, C. R., & Ewertowski, M. (2015). Controls on the location, morphology and evolution of complex esker systems at decadal timescales, Breidamerkurjökull, southeast Iceland. *Earth Surface Processes and Landforms*, *40*(11), 1421–1438. https://doi.org/10.1002/esp.3725

Storrar, R.D., Stokes, C.R. and Evans, D.J. (2013) A map of large Canadian eskers from Landsat satellite imagery. *Journal of maps*, *9*(3): 456-473

Storrar, R.D., Stokes, C.R. and Evans, D.J. (2014a) Morphometry and pattern of a large sample (> 20,000) of Canadian eskers and implications for subglacial drainage beneath ice sheets. *Quaternary Science Reviews*, *105*: 1-25

Storrar, R.D., Stokes, C.R. and Evans, D.J. (2014b) Increased channelization of subglacial drainage during deglaciation of the Laurentide Ice Sheet. *Geology*, *42*(3): 239-242

Stroeven, A. P., Hättestrand, C., Kleman, J., Heyman, J., Fabel, D., Fredin, O., Goodfellow, B. W., Harbor, J. M., Jansen, J. D., Olsen, L., Caffee, M. W., Fink, D., Lundqvist, J., Rosqvist, G. C., Strömberg, B. & Jansson, K. N. (2016) Deglaciation of Fennoscandia. *Quaternary Science Reviews*, 147, 91-121.

Warren, W.P. and Ashley, G.M. (1994) Origins of the ice-contact stratified ridges (eskers) of Ireland. *Journal of Sedimentary Research*, *64*(3a): 433-449

940 Wilson, P., Ballantyne, C.K., Benetti, S., Small, D., Fabel, D. and Clark, C.D., 2019. Deglaciation
941 chronology of the Donegal Ice Centre, north-west Ireland. Journal of Quaternary Science,
942 34(1), pp.16-28

943

944 Winsemann, J., Asprion, U., Meyer, T. and Schramm, C. (2007) Facies characteristics of Middle
945 Pleistocene (Saalian) ice-margin subaqueous fan and delta deposits, glacial Lake Leine, NW
946 Germany. *Sedimentary Geology*, *193*(1-4): 105-129

947 Wright, A. P., Siegert, M. J., Le Brocq, A. M., & Gore, D. B. (2008). High sensitivity of subglacial
948 hydrological pathways in Antarctica to small ice-sheet changes. *Geophysical Research*
949 *Letters*, *35*(17), 1–5. https://doi.org/10.1029/2008GL034937

950 Zwally, H.J., et al. (2002). Surface melt-induced acceleration of Greenland ice-sheet flow. Science,
951 297(5579), 218-222.

952

953

954